Control of telomere length in yeast by SUMOylated PCNA and the Elg1 PCNA unloader

Pragyan Singh, Inbal Gazy and Martin Kupiec*

[1]The Shmunis School of Biomedicine and Cancer Research, The George S. Wise Faculty of Life Sciences, Tel Aviv University, Tel Aviv 69978, Israel

***Corresponding author: martin@tauex.tau.ac.il**

ABSTRACT

Telomeres cap and protect the linear eukaryotic chromosomes. Telomere length is determined by an equilibrium between positive and negative regulators of telomerase activity. A systematic screen for yeast mutants that affect telomere length maintenance in the yeast *Saccharomyces cerevisiae* revealed that mutations in any of ~500 genes affects telomere length. One of the genes that, when mutated, causes telomere elongation is *ELG1*, which encodes an unloader of PCNA, the processivity factor for replicative DNA polymerases. PCNA can undergo SUMOylation on two conserved residues, K164 and K127, or ubiquitination at lysine 164. These modifications have already been implicated in genome stability processes. We report that SUMOylated PCNA acts as a signal that positively regulates telomerase activity. We also uncovered physical interactions between Elg1 and the CST (Cdc13-Stn1-Ten) complex, and dissected the mechanism by which Elg1 and Stn1 negatively regulates telomere elongation, coordinated by SUMO. We present a model that provides mechanistic insights on how chromosomal replication and telomere elongation are coordinated.

INTRODUCTION

Telomeres cap the ends of linear eukaryotic chromosomes and safeguard them against genome instability. Telomeric DNA consists of G/C-rich DNA repeats, with the G-rich strand extending to form a 3' single-stranded overhang. Telomeres are primarily involved in counteracting the gradual shortening of the telomeric DNA caused by conventional DNA replication, thereby solving the “end-replication problem” (Bonnell, Pasquier, & Wellinger, 2021; Soudet, Jolivet, & Teixeira, 2014). Another important function of telomeres is to protect chromosome ends from improper recognition as a DNA double-strand break (DSB) [reviewed in (de Lange, 2018)].

An important, conserved protein complex involved in regulation of telomere length is the CST, which in *Saccharomyces cerevisiae* is composed of Cdc13, Stn1, and Ten1 (L. Y. Chen & Lingner, 2013; Ge et al., 2020; Lim et al., 2020; Puglisi, Bianchi, Lemmens, Damay, & Shore, 2008; Rice & Skordalakes, 2016). The CST has similarity to the ssDNA binding complex RPA and localizes specifically to the single-stranded telomeric DNA, where it is involved in chromosome end capping and telomere length regulation (Hughes, Weilbaecher, Walterscheid, & Lundblad, 2000; Lin & Zakian, 1996; Mersaoui & Wellinger, 2019). The CST facilitates telomerase-mediated telomere elongation (Evans & Lundblad, 1999, 2000; Nugent, Hughes, Lue, & Lundblad, 1996), participates in telomere processing during DNA replication (Soudet et al., 2014), and helps “capping” the telomere (Mersaoui & Wellinger, 2019). In late S-phase Cdc13 interacts with the Est1 subunit of telomerase and promotes telomerase activity (Chandra, Hughes, Nugent, & Lundblad, 2001; H. Chen et al., 2018). Stn1 binds Cdc13 in a region that overlaps with that bound by Est1. Recruitment of Stn1 evicts Est1 and prevents further elongation of the G-strand (Chandra et al., 2001; Wang et al., 2000). The amino terminus of Stn1 binds Ten1, whereas its C-terminus interacts with both Cdc13 and Pol12, a subunit of Polymerase Alpha (Grossi, Puglisi, Dmitriev, Lopes, & Shore, 2004; Petreaca et al., 2006; Puglisi et al., 2008). Thus, the CST coordinates leading strand elongation by telomerase with lagging strand DNA synthesis by the cell's replisome (Grossi et al., 2004).

Very often the integrity of the genome is compromised by internal and external sources of DNA damage. This vulnerability increases during S-phase, when the DNA is unpacked and copied. Elg1, the major subunit of a replication factor C-like complex (RLC), plays a central role in DNA replication and is critical for genome maintenance. In *Saccharomyces cerevisiae*, loss of the *ELG1* gene causes gross chromosomal rearrangements, chromosome losses, defective sister chromatid cohesion and recombination, increased sensitivity to DNA damaging agents and abnormal telomere length maintenance [reviewed in (Arbel, Choudhary, Tfilin, & Kupiec, 2021)]. The function of the Elg1 RLC is to unload the processivity factor PCNA from chromatin, in particular after Okazaki fragment processing and ligation in the lagging strand, and during DNA repair (Kubota, Katou, Nakato, Shirahige, & Donaldson, 2015; Kubota, Nishimura, Kanemaki, & Donaldson, 2013; Parnas et al., 2010; Shemesh et al., 2017). The mammalian ortholog of *ELG1* (ATAD5) participates in the Fanconi Anemia pathway (Kim et al., 2020; Yang et al., 2011) and, when mutated, leads to genome instability and cancer in mice and humans (Bell et al., 2011; Kuchenbaecker et al., 2015; Maleva Kostovska et al., 2016).

Post-translational modifications of PCNA (in particular ubiquitination and SUMOylation) orchestrate the activity of a large number of interacting proteins during DNA replication and repair. Many of these proteins interact through a PIP (PCNA Interacting Peptide) motif. PCNA can undergo SUMOylation on two conserved residues, K164 and K127, or ubiquitination at lysine 164. Although the Elg1 RLC shows affinity to SUMOylated PCNA, the complex is able to unload modified and unmodified versions of the clamp (Kang et al., 2019; Kubota et al., 2015; Kubota et al., 2013; Parnas et al., 2010; Shemesh et al., 2017; Shiomi & Nishitani, 2013). Thus SUMOylation may assist but is not essential for PCNA unloading. Retention and accumulation of PCNA on DNA is the major cause of genome instability in *elg1Δ* (Itzkovich, Choudhary, Arbel, & Kupiec, 2023; Johnson, Gali, Takahashi, & Kubota, 2016; Shemesh et al., 2017).

Previous studies found that telomeric proteins, and in particular the CST, can be regulated by SUMO modification (Hang, Liu, Cheung, Yang, & Zhao, 2011). Here we show that SUMOylation of PCNA plays a role in the regulation of telomere length, and uncover an interaction between the Elg1 RLC and the CST. We report that PCNA SUMOylation

positively regulates telomerase activity, and its unloading by the Elg1-RLC is essential for normal telomere size regulation. The N-terminus of Elg1 interacts with Stn1 during late S phase, and mediates the interaction between Stn1 and Cdc13 after PCNA has been unloaded from the telomeres.

RESULTS

The long telomeres phenotype of *elg1*Δ strains requires PCNA SUMOylation

Previous results suggested that the Elg1 protein preferentially interacts with the SUMO machinery, and with SUMOylated PCNA (Parnas, Amishay, Liefshitz, Zipin-Roitman, & Kupiec, 2011; Parnas et al., 2010; Shemesh et al., 2017). To test whether PCNA modifications play any role in the elongated telomere phenotype of *elg1Δ*, we combined the *ELG1* deletion with mutations in the *POL30* gene, encoding PCNA. We mutated either lysine 127, lysine 164, or both (hereafter referred as *pol30-K127R, pol30-K164R,* and *pol30-RR*, respectively) in the *elg1*Δ background. **Figure 1** shows that the mutations in *POL30* have little effect by themselves. Importantly, whereas the single mutants did not affect the long telomeres of *elg1*Δ, mutating both lysine residues of each PCNA subunit completely abrogated the long telomere phenotype. Lysine 164 can be modified by both SUMO and ubiquitin; mutating only this residue prevents ubiquitination, but not SUMOylation; figure 1demonstrates that this mutant shows no effect. To ensure that SUMO, and not ubiquitin, is the modification responsible for the long telomeres of *elg1*Δ, we deleted *RAD18*, encoding the E3 ubiquitin ligase required to ubiquitinate PCNA (Hoege, Pfander, Moldovan, Pyrowolakis, & Jentsch, 2002; Stelter & Ulrich, 2003). Figure 1 shows that lack of Rad18 has no effect on the elongated telomeres of *elg1*Δ. [Deletion of the SUMO E3 ligases *SIZ1* and *SIZ2* (to prevent SUMOylation) by itself alters telomere length (Hang et al., 2011) and thus they could not be used here]. We conclude that SUMOylation of PCNA is required for the long telomeres phenotype of *elg1*Δ mutants.

These results suggest that SUMOylated PCNA may play a central role in determining telomere length also in cells with wild type Elg1 activity. We thus next asked whether artificially overexpressing modified and unmodified PCNA may mimic the long

121 telomere phenotype of *elg1*Δ. Since it is hard to force ubiquitination or SUMOylation
122 of PCNA *in vivo*, we used covalent fusions between PCNA and either ubiquitin or
123 SUMO. These have been shown in the past to mimic naturally modified PCNA
124 molecules (Parker, Bielen, Dikic, & Ulrich, 2007; Takahashi, Wollscheid, Lowther, &
125 Ulrich, 2020). We overexpressed either wild type Pol30, Pol30-RR (which cannot be
126 modified) or Pol30-RR fused either to ubiquitin or to SUMO, in *pol30-RR* cells, unable
127 to carry out modifications of the PCNA encoded by the genome. **Figure 1B** shows that
128 telomeres become elongated upon overexpression of the wild type protein (which
129 can be modified), or the Pol30-RR version fused to SUMO, but do not elongate upon
130 overexpression of the unmodifiable Pol30-RR version, or the one fused to ubiquitin.
131 These results, together with those of Figure 1A, show that ~~accumulation of~~
132 SUMOylated PCNA, and not unmodified or ubiquitinated PCNA, is both necessary and
133 sufficient for telomere elongation in the presence or in the absence of Elg1.

134 **Genetic and Physical interactions between Elg1 and Stn1**

135 The elongated telomere phenotype of Elg1 was identified in systematic screens of the
136 yeast knockout collection (Askree et al., 2004; Gatbonton et al., 2006), together with
137 ~200 additional mutants of similar phenotypes. To identify the pathway of telomere
138 length maintenance in which Elg1 participates, we systematically combined the *elg1*Δ
139 mutant with all the other mutants with long telomeres. Most double mutants
140 exhibited telomeres longer than each of the single mutants, indicating that they affect
141 different pathways. One of the mutants showing clear epistasis (the double mutant
142 was not longer than the single mutants) carried a deletion of *RRP8*, a gene involved in
143 modification of the ribosomal RNA. Further analysis demonstrated that the knockout
144 of *RRP8* exhibited the "neighboring gene effect", and in fact the deletion of *RRP8*
145 caused a decrease in the expression of its neighboring gene, *STN1* (Ben-Shitrit et al.,
146 2012). We confirmed the genetic interactions between *ELG1* and *STN1* alleles by
147 combining *elg1*Δ with the *stn1-13* and *stn1-164* alleles (Grandin, Reed, &
148 Charbonneau, 1997), which exhibit long telomeres. The telomeres of the double
149 mutants are not longer than those of the single mutants (**Figure 2A**), indicating that
150 Elg1 works in the same TLM pathway as Stn1.

Given the epistatic relations between the *ELG1* and *STN1* genes, we addressed, by co-Immunoprecipitation (IP) and Yeast-Two-Hybrid (YTH) assay, whether the proteins in the CST complex interact with Elg1. IP of epitope-tagged Elg1 pulled down Stn1 but not the other two members of the CST complex, Cdc13 or Ten1 (**Figure 2B**). For our YTH experiments, the Elg1 protein was divided into three main functional domains: an N-terminal domain (amino acids 1-234), a central AAA domain (amino acids 235-514) and a C-terminal domain (amino acids 515-791) (Itzkovich et al., 2023), **Figure 3A**. The AAA and C-terminal domains contain the conserved RFC boxes and are required for the interactions with the small RFC subunits, shared by all RFC-like domains. The N-terminal domain (hereafter referred to as NTD) is unique to Elg1 (Arbel et al., 2021). We thus concentrated on this domain, and used the C-terminus as a negative control, as it does not interact with any of the proteins tested here.

The NTD contains SUMO-interacting motifs (SIMs), which were previously shown to interact with SUMO and the SUMO machinery (Parnas et al., 2011; Parnas et al., 2010) (**Figure 3A**). We used the YTH technique to test potential interactions between Elg1 and the CST components, and their dependency on SUMO. The N-terminus of Elg1 interacted strongly with Cdc13 and Stn1, and weakly with Ten1 (**Figure 3B,C, Figure S1**). In contrast, no interaction was detected with Elg1's CTD. We could also detect interactions of Cdc13, Stn1 and Elg1's NTD with SUMO (Figure 3). These were used as positive controls in all our experiments. Since the results with Ten1 were much weaker than those with Cdc13 and Stn1, we concentrated on these two last proteins. Below, we dissect, using YTH in various genetic backgrounds, the interactions between Elg1, Stn1, Cdc13 and PCNA. The results are also summarized in **Table 1**.

Table1: Summary of all YTH interactions presented.

Strain	Plasmid	Interaction w/Stn1	Interaction w/Cdc13
wild type	Elg1-NTD	**YES**	**YES**
wild type	Elg1-sim	**NO**	**YES**
*siz1*Δ *siz2*Δ	Elg1-NTD	**NO**	**NO**

pol30-RR	Elg1-NTD	**YES**	**NO**
elg1Δ	Elg1-NTD	**YES**	**NO**
elg1-sim	Elg1-NTD	**YES**	**YES**
elg1-DD	Elg1-NTD	**YES**	**NO**
elg1-sim+DD	Elg1-NTD	**YES**	**NO**
elg1-WalkerA	Elg1-NTD	**YES**	**NO**
cdc13-snm	Elg1-NTD	**YES**	**YES**
wild type	Elg1-NTD	**-**	***snm:* NO**

elg1-sim: mutation in the SUMO-interacting motif of Elg1; *elg1-DD: TT386/7DD*; *elg1-sim+DD*: combination of mutations in the SIM and in TT386/7; *elg1-WalkerA*: mutation that eliminates ATPase and unloading activity of Elg1. *cdc13-snm:* allele of Cdc13 that cannot be SUMOylated.

Interestingly, the interaction of Elg1's NTD with Stn1, but not with Cdc13, was abolished when the SIM motifs (amino acids I27A, I93K, I121A, and I122A) were mutated (**Figure 3B,C**). We confirmed these results by co-Immunoprecipitation (co-IP) (**Figure 2B**). These results suggest that the interaction with Stn1 is mediated by SUMOylation of a protein, whereas the interaction of Cdc13 with Elg1-NTD is independent of the SIM in the plasmid-borne copy of Elg1. We confirmed this result by deleting the genes encoding the SUMO-specific E3 enzymes, *SIZ1* and *SIZ2* in the genome (a double deletion is necessary, as many times each protein can compensate for the lack of the other). **Figure 3D** shows that indeed, deletion of the genes encoding these enzymes abolishes the interaction of Stn1 and Cdc13 with Elg1's NTD. We conclude that SUMO plays a role in mediating the Elg1-CST interactions. Since Elg1 preferentially interacts with SUMOylated PCNA (Parnas et al., 2010), and Stn1 can bind SUMO non-covalently in YTH (**Figure 3C**), we reckoned that SUMOylated PCNA may mediate the interaction between Stn1 and Elg1. We therefore tested whether

196 abolishing PCNA's SUMOylation sites in the genome (*pol30-RR*) had an effect on the
197 Stn1-Elg1 interaction. We found, however, that Elg1 and Stn1 could still interact in
198 the *pol30-RR* strain (**Figure 3D**), despite the fact that PCNA cannot become
199 SUMOylated. Consequently, a different SUMOylated target seems to mediate the
200 interaction between Elg1 and Stn1, or else either one of the proteins is SUMOylated.
201 Despite numerous attempts, we were unsuccessful in observing SUMOylation of
202 either Stn1 or Elg1.

203 We also noted that, despite the fact that mutation in the plasmid-borne NTD's SIM
204 had no effect on the interaction with Cdc13 (**Figure 3B**), deletion of *SIZ1* and *SIZ2*,
205 and mutation in the SUMOylation sites in PCNA completely abolished the interactions
206 between Elg1's NTD and Cdc13 (**Figure 3D**). This implies that PCNA SUMOylation is
207 necessary for the interaction between Elg1 and Cdc13. We confirmed by co-IP that
208 Cdc13 indeed physically interacts with PCNA (**Figure 3E**). The interaction between
209 Cdc13 and PCNA was almost completely abolished when PCNA could not be
210 SUMOylated (Figure S2), In summary, the interaction between Cdc13 and both PCNA
211 and Elg1, but not that of Elg1 with Stn1, is dependent on SUMOylation of PCNA.**Elg1's**
212 **functional activity is essential for its interaction with Cdc13**

213 When we repeated the YTH assays in a strain in which the *ELG1* gene is deleted from
214 the genome, we were surprised to see that now Cdc13 failed to interact with the
215 plasmid-borne Elg1-NTD (**Figure 4A**, compare to Figure 3B). In contrast, the
216 interaction between Stn1 and Elg1-NTD was not affected by the deletion of the
217 genomic *ELG1*.

218 Taken together, these results imply that whereas Stn1 interacts directly with the
219 plasmid-borne Elg1-NTD, via its SIM-mediated SUMO-binding, the interaction with
220 Cdc13 require both PCNA SUMOylation and the genomic *ELG1* gene. We can envision
221 two formal possibilities for the latter requirement: either 1) the interaction with
222 Cdc13 requires parts of the Elg1 protein not present in the plasmid-borne NTD (e.g.,

223 the AAA or CTD domain), or 2) Elg1's activity (e.g., PCNA unloading) may be required
224 to facilitate the physical interaction of the NTD with Cdc13.

225 To distinguish between these two possibilities, we carried out YTH experiments with
226 strains carrying different alleles of *ELG1* in the genome. Three mutations were tested
227 first: *elg1-sim* (mutated in amino acids I27A, I93K, I121A I122A), which does not
228 interact with SUMO; *elg1-TT386/387DD*, hereafter referred to as *elg1-DD*, which
229 affects the interface Elg1-PCNA (Shemesh et al., 2017); and *elg1-sim+DD*, an allele that
230 combines both mutations. Whereas the *SIM* mutation has a very mild effect on the
231 ability of cells to unload PCNA, and displays no phenotypes, the *elg1-DD* is more
232 impaired and has a stronger phenotype, and the *elg1-sim+DD* allele has essentially a
233 null phenotype, similar to that of *elg1*Δ, but expressing the protein at normal levels
234 (Itzkovich et al., 2023; Shemesh et al., 2017).

235 We found that in strains carrying genomic *elg1-DD* and *elg1-sim+DD* alleles, Cdc13
236 failed to interact with plasmid borne Elg1-NTD, whereas in the *elg1-sim* strain the
237 interaction was weak but clearly seen (**Figure 4B-D**). This observation indicates that
238 the PCNA unloading activity of Elg1 is essential to allow the interaction between
239 Cdc13 and the plasmid borne Elg1-NTD: this activity is high in *elg1-sim* mutants,
240 intermediate in the *elg1-DD* strain and is abolished by the *elg1-sim+DD* mutations.
241 Note that the presence of a functional SIM at the plasmid-borne NTD is sufficient to
242 ensure a mild interaction with Cdc13, but only if the genomic copy retains PCNA
243 unloading activity (as in the *elg1-sim* mutant). On the other hand, the presence of a
244 functional SIM in the inactive *elg1-DD* allele does not warrant an interaction of Elg1's
245 NTD (which has SIM motifs) with Cdc13. We confirmed this idea by analyzing the
246 interaction between Cdc13 and Elg1's NTD in another SIM-containing mutant strain
247 devoid of PCNA unloading activity, *elg1-WalkerA* (KK343/4DD), which lacks ATPase
248 and PCNA unloading activity (Itzkovich et al., 2023). This mutant expresses wild type
249 levels of protein, and the mutant has essentially the same phenotype of an *elg1*Δ allele.
250 **Figure 4E** shows that no interaction between the plasmid-borne Elg1 NTD and Cdc13
251 could be detected, despite the fact that functional SIMs are present both at the NTD

252 and in the genome-encoded Elg1-WalkerA protein. All the mutants expressed the Elg1
253 protein at wild type levels (**Figure S3**).

254 We conclude that whereas the interaction with Stn1 is direct and mediated by the
255 SUMOylation of a protein (different from PCNA), the interaction between Elg1's NTD
256 and Cdc13 is indirect, and can only take place after PCNA has been SUMOylated and
257 unloaded. This suggests a model for the coordination of telomerase activity and DNA
258 replication: the presence of SUMOylated PCNA at telomeres may serve as a positive
259 signal for telomerase activity. Once Elg1 unloads PCNA, however, Stn1-Elg1 can bind
260 Cdc13, ending telomerase activity. In this context, it is possible to understand the
261 results seen in **Figure 3**D, showing that mutations in the SUMO E3 enzymes or in the
262 sites of SUMOylation of PCNA, both of which prevent PCNA SUMOylation, show the
263 same effect as the *sim+DD* or *walkerA* mutations in the genomic *ELG1* copy, which
264 prevent PCNA unloading activity.

265 **SUMOylation of Cdc13 is needed for interaction with Elg1**

266 Cdc13 undergoes SUMOylation, and this modification plays an essential role in the
267 negative regulation of telomere length (Hang et al., 2011). Thus, Cdc13 is a good
268 candidate for the target of SUMOylation required for the interaction between Elg1
269 and Stn1. Accordingly, mutations of the Cdc13 SUMOylation sites (*cdc13-snm*, "SUMO
270 no more") weaken its interaction with Stn1 and lead to elongated telomere phenotype
271 (Hang et al., 2011). We therefore checked whether the *cdc13-snm* mutation affects
272 also the interaction with Elg1. **Figure 4F** shows that indeed preventing SUMOylation
273 of Cdc13 abolishes the interaction between this protein and Elg1. Note that the strain
274 used expresses a wild type genomic copy of *CDC13*. Thus, SUMOylation **of the**
275 **plasmid-borne version of Cdc13** (i.e., in *cis*) is required for these interactions in the
276 YTH assay. No effect was observed when the YTH plasmid carried a wild type copy of
277 *CDC13*, and the genomic copy was the *cdc13-snm* allele (**Figure S4A**). In summary, the
278 N-terminus of Elg1 interacts with Cdc13 only if 1) Cdc13 can be SUMOylated (**Figure**
279 **4F**), 2) PCNA can be SUMOylated (**Figure 3**D), and 3) PCNA can be unloaded (**Figure**
280 **4A, C, D,E**).

281 **The interaction of Elg1 with Stn1 takes place only at late S-phase**

282 The fact that the interactions of the Elg1 NTD with Cdc13 are dependent on PCNA
283 modification and unloading, whereas those with Stn1 are not, suggests that the
284 interaction with Cdc13 may be mediated by, or dependent on, the interaction of Elg1
285 with Stn1. To further dissect this point, we divided the Stn1 protein into an NTD (first
286 281 amino acids) and a CTD (amino acids 282-495). The later has been shown to be
287 the region that interacts with Cdc13 (Petreaca, Chiu, & Nugent, 2007). **Figure S4B**
288 shows that the NTD of Elg1 also interacts with Stn1 via its C-terminal domain, both in
289 *WT* and *elg1*Δ strains.

290 Having established Stn1 as the main interactor of Elg1 in the CST complex, we next
291 examined the interaction between these proteins throughout the cell cycle phases.
292 We arrested a strain with tagged Elg1, Stn1 and DNA Polymerase Delta in G1 with
293 alpha factor. Cells were released into the cell cycle and samples were taken at
294 intervals during two cell cycles. This allowed us to map the timing of interaction
295 between Elg1 and Stn1 proteins, and whether this interaction is codependent on the
296 movement of replication fork. **Figure S5** shows that the total level of these proteins
297 does not change throughout the cell cycle. We immunoprecipitated Elg1, and
298 measured the level of the other two proteins by Western blot (**Figure 5A-C**). Pol3 was
299 co-IPed with Elg1 strongly only during the S phase (40-70 minutes, 120-140 minutes)
300 whereas Stn1 was only detected in late S phase (60-70 minutes, 140-160 minutes) for
301 both cell cycles and was barely detected in G1 (**Figure 5A-C**). This pattern coincides
302 with telomerase activity at telomeres, which is low in early to mid S phase and peaks
303 in late S-phase (Bianchi et al., 2008, Giraud et al., 2008, Taggart et al., 2002).

304 To monitor the arrival of the replication fork to telomeres, we performed chromatin
305 immunoprecipitation at telomeres (Telo-ChIP) in synchronized cells. **Figure 5D**
306 shows that the timing of arrival of PCNA to the telomeres (60-70 minutes into the cell
307 cycle) coincides with the timing of the co-IP between Elg1 and Stn1 (**Figure 5A-C**).
308 Thus, our results are consistent with the idea that Elg1 moves with the replication

309 fork, and interacts with Stn1 at the end of S-phase, when telomeres are replicated and
310 telomerase is activated.

311 **The interaction between Cdc13 and Stn1 is dependent on Elg1**

312 Our YTH and IP data suggest that unlike the relationship between Cdc13 and Elg1, the
313 interaction between Stn1 and Elg1 is direct (**Figures 2 and 3**). Since both Elg1 and
314 Cdc13 bind Stn1 at its C-terminus [**Figure S3** and (Petreaca et al., 2007)], it is possible
315 that the absence of Elg1 may affect the interaction between the two CST members.
316 We thus measured the co-IP of Cdc13 and Stn1 in a wild type or an *elg1*Δ strain. Cells
317 were cell-cycle synchronized in S-phase, as the interaction between these two
318 proteins was barely seen when immunoprecipitated in an asynchronous culture.
319 When Elg1 was absent, Stn1 exhibited a strong reduction in its co-precipitation with
320 Cdc13 (**Figure 5E,F**). This suggests that the interaction between Stn1 and Cdc13 is,
321 at least partly, dependent on Elg1.

322 **Model: Elg1 negatively regulates the telomere length by forming an**
323 **interaction with the CST complex**

324 Taken together, our results suggest the following model (**Figure 6**):

325 Following firing of the origin proximal to the telomeres at late S-phase, Elg1 moves
326 with the fork, unloading PCNA from the lagging strand as the fork progresses (Kubota
327 et al., 2015; Kubota et al., 2013; Shemesh et al., 2017) (**Figure 6A**). SUMOylation of
328 PCNA acts as a signal for the activation of telomerase (**Figures 1A,B and 6B**). Once
329 Elg1 reaches the telomeres, it interacts with Stn1 (**Figure 5**). This interaction
330 requires SUMOylation of Stn1 or of some other protein, which is not PCNA (**Figure**
331 **3D**) nor Cdc13 (**Figure S3A**) and could be Stn1 itself or another telomeric protein
332 (Hang et al., 2011). The Elg1-Stn1 complex then unloads the SUMOylated PCNA at the
333 telomeres, and Cdc13 becomes SUMOylated (**Figure 6C**), now interacting with Elg1-
334 Stn1. SUMOylation of Cdc13 allows its interaction with Stn1, and presumably with
335 Ten1 (Hang et al., 2011), creating the complete CST complex, and preventing further
336 telomerase activity (**Figure 6D**). The fact that co-IP experiments detect a strong

interaction with Stn1 but fail to detect an interaction with Cdc13 (**Figure 2B**) suggests that indeed the interaction Elg1-Cdc13 is very transient, and Elg1 leaves chromatin immediately, leaving the C-terminus of Stn1 free to interact with Cdc13. It is possible that a single "wave" of SUMOylation at the telomeres coordinates PCNA unloading with the interaction between Elg1 and Cdc13. Alternatively, unloading of PCNA by Elg1 may allow the recruitment of SUMO ligases to modify Cdc13. In support for this idea, YTH interactions between Stn1 or Cdc13 with SUMO are abolished in *siz1*Δ *siz2*Δ strains (**Figure 3**D).

DISCUSSION

We have presented evidence for the fact that two negative regulators of telomerase activity, Elg1 and Stn1, work in the same pathway to coordinate chromosomal DNA replication and telomere elongation. We present a model (**Figure 6**) in which the unloading of SUMOylated PCNA by Elg1 at telomeres facilitates the interaction between Stn1 and Cdc13 that negatively regulate telomerase activity.

This model is supported by several observations. First, the double mutants of Elg1 and Stn1 do not show increased telomere length phenotype in comparison to the single mutants, indicating that both proteins work in the same pathway that negatively regulates telomere length (**Figure 2A**). In addition, the interaction between Elg1 and Stn1 seems direct and occurs exclusively during the late S-phase (**Figures 2B** and **5A-C**). This interaction is neither dependent on SUMOylation of PCNA (**Figure 3D**) nor on Cdc13 (**Figure S3A**). In contrast, the interaction between Cdc13 and Elg1 is dependent on both the SUMOylation of PCNA (Figure 3**D**) and of Cdc13 itself (**Figure 4F**). We suggest that Elg1 participates in the negative regulation of telomere length by unloading SUMOylated PCNA from the telomeres. This eliminates a positive signal for telomerase activity, and causes the exchange of Est1 by Stn1 as interactor of Cdc13, effectively terminating telomerase activity (Chandra et al., 2001; Gao, Cervantes, Mandell, Otero, & Lundblad, 2007; Ge et al., 2020; Hang

365 et al., 2011; Puglisi et al., 2008). As expected from the model, the interaction Elg1-
366 Cdc13 is transient, and cannot be detected by co-IP.

367 We present evidence for the fact that SUMOylated PCNA serves as a positive signal for
368 telomere elongation (**Figure 1**). Preventing its unloading (by mutations in the *ELG1*
369 gene) leads to elongated telomeres, and so does PCNA overexpression, provided the
370 protein is able to be SUMOylated, or is fused to SUMO (thus mimicking SUMOylated
371 PCNA) (**Figure 1**). *ELG1* is the only PCNA unloader in eukaryotes; however, it is not
372 an essential gene, implying that there are alternative ways in which PCNA can get
373 unloaded (either spontaneously or with the help of RFC) (Arbel et al., 2021). Once this
374 step does take place, Stn1 can replace Est1 as Cdc13's partner, and stop the activity
375 of telomerase, but at a longer telomere steady state equilibrium point. This explains
376 both the long telomere phenotype of *elg1* mutants, and the fact that it is less severe
377 than that of *stn1* alleles (**Figure 2**). The fact that *pol30-RR* mutants have stable,
378 normal-sized telomeres (**Figure 1**), imply that despite lacking PCNA SUMOylation,
379 they are able to solve the "end replication problem". Our results support the notion
380 (Maicher et al., 2017) that there are two alternative modes of telomerase: one
381 carrying "basal activity", with minimal genetic requirements, able to maintain most
382 telomeres at normal size, and another, "sustained activity", required for increased
383 elongating activity (Maicher et al., 2017). Previous results have shown that the first
384 mode does not require Rnr1, the large subunit of the ribonucleotide reductase
385 enzyme, whereas the second depends on it (Maicher et al., 2017). Similarly,
386 SUMOylated PCNA is only needed for the second mode of telomerase. In our
387 experiments, the phenotype that we monitored was elongated telomeres (e.g., by
388 deletion of *ELG1* or by overexpression of PCNA) which required sustained telomerase
389 activity. To solve the “end replication problem” and maintain normal telomere length,
390 very little telomerase activity might be needed, and even unmodified PCNA or
391 telomeric proteins might be able to provide that basal level.

392 Many proteins in the cell become SUMOylated at one point or another. This
393 modification is usually transient, due to the activity of de-SUMOylases (which
394 eliminate the modification) and STUbLs (SUMO-dependent ubiquitin ligases, which

usually send the protein to degradation). It has been proposed that SUMOylation often works by targeting many physically interacting proteins together. This may be executed by the local recruitment of SUMO ligases to preassembled, co-localized protein groups. SUMOylation thus may increase their interactions, acting to increase their local concentration or effective interaction (Jentsch & Psakhye, 2013). SUMOylation of telomeric proteins seems to be one of those cases (Garg et al., 2014; Hang et al., 2011; Matmati et al., 2018; Miyagawa et al., 2014). In our model, PCNA, Cdc13 and possibly Stn1 undergo SUMOylation to ensure the proper sequence of events in the coordination between telomerase activity and chromosomal replication. Cdc13 binds Pol12, a subunit of Polymerase Alpha (Grossi et al., 2004; Petreaca et al., 2006; Puglisi et al., 2008), allowing the synthesis of the lagging strand on the newly synthesized ssDNA. Thus, the arrival of the replisome to a short telomere at the end of S-phase brings PCNA, whose SUMOylation can elicit both telomerase activity, and its subsequent repression when PCNA is unloaded by Elg1. This in turn primes synthesis of the complementary strand, thus coordinating telomere elongation with chromosomal replication.

MATERIALS AND METHODS

Yeast strains, plasmids and Media: All yeast strains used are described in **Table 2**. All plasmids are described in **Table 3.** Yeast extract-peptone-dextrose (YPD) medium was prepared with a ready-to-use mixture (Formedium). Synthetic complete (SC) minimal medium was prepared with 2% dextrose (Formedium), yeast nitrogen base without amino acids (Difco), and all necessary amino acids. 2% agar (Difco) was added for solid medium. Standard yeast genetic procedures were used to create single and double mutants. Unless stated otherwise, all experiments were carried out at 30ºC.

PCNA overexpression: The high copy number pGAD424 plasmid alone, or carrying the wild type *POL30*, the mutant *pol30-KK127,164RR* (*pol30-RR*), or the *pol30-RR* fused to ubiquitin or to SUMO (Parker et al., 2007; Takahashi et al., 2020) were transformed into *pol30-RR* strains and grown under selective conditions.

424 **Southern Teloblots** (Harari & Kupiec, 2018; Harari, Romano, Ungar, & Kupiec, 2013;
425 Harari, Zadok-Laviel, & Kupiec, 2017; Rubinstein et al., 2014): For each genotype, at
426 least 3 independently created strains were tested after 10 consecutive passages on
427 YPD plates. Genomic DNA was isolated by pelleting 15 ml saturated overnight yeast
428 culture grown in YPD, then beating the cells using 0.5 mm glass beads in 500 µl lysis
429 buffer and 500 µl phenol chloroform. Cells were spun down for 10 min at 14 000 rpm,
430 and ~500 µl of the top clear solution, containing the genomic DNA, was carefully
431 taken out. DNA was precipitated using 1000 µl of 95% ethanol and then pelleted. The
432 supernatant was discarded, and 500 µl of 70% ethanol was added. Pellets were left to
433 dry before resuspension in 300 µl TE with RNaseA for 10 minutes at 65°C. The DNA
434 was precipitated by adding 130 µl of 7.5 M ammonium acetate (pH 7) and 1 ml of 95%
435 ethanol at −20°C, spun, and resuspended in 50 µl of TE. About 10 µl of genomic DNA
436 was digested using XhoI overnight at 37°C. Digested gDNA and ladder were loaded
437 onto a 0.8% agarose gel and electrophoresed overnight at ~67V in 1X TBE. The gel
438 was denatured for 30 min in a rocking shaker (1.5 M NaCl, 0.5 M NaOH) and was
439 neutralized for 15 min (1.5 M NaCl, 0.5M Tris, pH 7.0). The DNA on the gel was
440 transferred onto a hybond nylon membrane (GE Healthcare GERPN303B) with 10X
441 SSC (1.5 M NaCl 0.17 M NaCitrate, dihydrate) and UV cross-linked before blocking in
442 Church buffer (0.5 M Na_2HPO_4, pH7.2, 7% SDS, 1 mM EDTA, 1% BSA) for ~2 h at
443 65°C. ^{32}P radiolabeled PCR fragments were added onto the membrane and left to
444 incubate overnight. The membrane was washed 3–4 times for 15 min each, with 1X
445 SSC 0.1%SDS buffer before drying and exposing it to X-ray film. The teloblots blots
446 were exposed for 1-8 days at -70°C before the film was developed.

447 **Telomeric probe**: S. cerevisiae-specific telomeric probe was labeled by random
448 priming of 20 -25 ng of a telomeric fragment and of 20-25 ng of size-control fragments
449 using the DNA labeling mix from Biological Industries. Both fragments were
450 generated by PCR using the primers indicated below. For the telomeric probe, a
451 specific region of the left telomere of chromosome VII was amplified to generate a
452 product 370 bp long. As size-control probe, a specific region of chromosome II was

amplified to generate a product 1100 bp long. Since it contains an XhoI site, the size-control probe detects two bands in the sizes of 2044bp, 779bp in the Southern blot.

The primers for the Y' element product are:

Y' elementForward: GTTGGAGTTTTTCAGCGTTTGC

Y' element Reverse: TGTGAACCGCTACCATCAGC

The Y' element PCR product is ~370bp

The primers for the Control product are:

Tel Control Forward: TTGTAGGGGCCTTTTGTAATGT

Tel Control Reverse: GTGCGCCCAGTAAGGGGT

The Control PCR product is ~1100bp

Telomere length was determined using TelQuant (Rubinstein et al., 2014).

Yeast Two-Hybrid: The yeast two-hybrid assays were performed using PJ69-4A (James, Halladay, & Craig, 1996) strains cotransformed with a *LEU2*-marked plasmid containing genes fused to the *GAL4* activating domain (pACT or pGAD424) and a *URA3*-marked plasmid containing genes fused to the *GAL4* DNA binding domain (pGBU9). Strains containing the test plasmids were grown for 24 h at 30°C in SC-Ura-Leu liquid medium, and were plated on the reporter maker SC-His medium.

Protein extraction and immunoprecipitation (IP) assays: Cells were grown to mid-logarithmic phase, washed once with water, and resuspended in lysis buffer (20 mM Tris-HCl, pH 7.5, 0.5 mM EGTA, 0.5 mM EDTA, 1 mM DTT, 125 mM potassium acetate, 12.5% glycerol, 0.1% Triton X-100, protease inhibitor mixture, and 1 mM phenylmethylsulfonyl fluoride). Cells were broken for 45 min with glass beads, centrifuged for 10 min at 10,000 × *g* and the supernatant was collected. 20-30 μg of total protein extract was resolved on SDS-PAGE using 10% acrylamide

478 gels. For immunoprecipitation, 1,000 μg of proteins were prepared and pre-cleared
479 with 20 μl of protein A-Sepharose and protein G-Sepharose beads mixture (GE
480 Healthcare). 2 μl of (HA, Santa Cruz Biotechnology (sc7392; 1:1,000) or MYC, Santa
481 Cruz Biotechnology (9E10, SC-40; 1:1,000)) antibodies were added to the cleared
482 extract and incubated overnight at 4 ^{0}C. The beads were washed once with lysis
483 buffer, once with lysis buffer containing 0.5 M NaCl, and twice with buffer A (50
484 mM Tris-HCl, pH 7.5, 0.1 mM EGTA, 0.1% β-mercaptoethanol). The resulting
485 immunoprecipitates were used for *in vitro* kinase assays.

486 **Western blotting:** Cells were collected by centrifugation, re-suspended in 600 ul
487 of phosphate-buffered saline with 1% Triton X-100 (PBST), supplemented with a
488 protease inhibitor cocktail (Roche) and subjected to mechanical rupture using glass
489 beads. The cell debris were removed by centrifugation, and the supernatants were
490 applied onto 0.1 M dithiothreitol, and incubated at 80 ◦ C for 10 min before sodium
491 dodecyl sulphate-polyacrylamide gel electrophoresis (SDS-PAGE) (Resolving gel:
492 30% Acrylamide, 1.5 M Tris-HCl pH8.8, 10% SDS (pH 7.2), 9.7 ml H2O, 100 ul 10%
493 APS and 10 ul TEMED. Stacking gel: 30% Bis/Acrylamide, 1 M Tris-HCl pH 6.8, 10%
494 SDS (pH 7.2), 5.5 ml H2O, 800 ul 10% APS and 8 ul TEMED). The samples were run
495 with SDS-PAGE buffer at 100 V until the samples have passed the stacking gel and
496 then at 160 V until the samples have been fully separated. Transfer to nitrocellulose
497 was done in transfer buffer (200 ml Methanol, 3.03 gr Tris Base, 14.4 gr Glycine) at
498 500 mAmp and verified by staining with Ponceau-S dye. The blot was blocked with
499 Milk for at least 60 min at room temperature. Primary antibody was added for 12 h
500 at 4 ◦ C. The blot was washed 3 × 5 min with TBST (Tris-Buffered Saline Tween-20)
501 and secondary antibody was added for 1 h. The blot was washed 3 × 5 min with TBST
502 and subjected to electro-chemi-luminiscence (ECL).

503 **Cell cycle synchronization:** To assay Elg1 and Stn1 interaction during the cell
504 cycle, the triple tagged strain was grown in YPD to OD_{600} 0.6-0.8, followed by the
505 addition of 500ng/ml α factor and was grown until ~90% of the cells appeared

506 unbudded or exhibit Shmoo formation (for ~2 hrs). The α-factor was removed by
507 centrifugation and washing cells 2-3 times with warm YPD. Cells were released into
508 YPD at OD_{600} 0.6-0.8 with addition of pronase at a final concentration of 0.1mg/ml.
509 Cells were collected for both FACS and Western blot analysis at different time points
510 after release. Cells for FACS analysis were fixed in 70% ethanol, digested with RNase
511 overnight, washed again and stained with propidium iodide (15 μg/mL), and
512 analyzed by flow cytometry.

513 **Flow cytometry:** 200 μl of a logarithmic cell culture (0.6 OD600) were harvested,
514 resuspended in 60 μl of 50 mM Tris pH 7.5 and 140 μl of ethanol was added; cells
515 were then kept overnight at 4 °C. Fixed cells were centrifuged and washed once in
516 200 μl of 50 mM Tris pH 7.5 bufer and resuspended in 100 μl RNAse (0.2 mg/ml in
517 50 mM Tris pH 7.5) for 2 h at 37 °C. In addition, proteinase-K (0.2 mg/ml in 50 mM
518 Tris pH 7.5) was added to each tube and cells were incubated for 60 additional
519 minutes at 50 °C. 20 μl of the sample was taken into a new tube and a 180 μl of
520 18 μg/ml propidium iodide 50 mM Tris pH 7.5 was added. The samples were kept in
521 the dark at 4 °C overnight, sonicated twice at low setting (20% power) for 3–5 s and
522 stored in the dark at 4 °C. The fow cytometry MACSQuant system was used for
523 reading. Results were analyzed using either the Flowing Software or the FlowJo
524 program.

525 **Chromatin Immunoprecipitation:** 50 ml of each strain were grown to OD600
526 ≈ 1 in YPD. 1.5ml formaldehyde (37% solution) was added for 15 minutes and the
527 formaldehyde was quenched with 2.5ml of 2.5M glycine for five minutes. Cells were
528 harvested, washed once with 15ml cold PBS and broken down for 10 minutes with
529 glass beads in 600 μl lysis buffer (50mM HEPES-KOH pH7.5, 140mM NaCl, 1mM
530 EDTA, 1% triton X100, 0.1% Na-Deoxycholic acid). The supernatant (lysate) was
531 removed to a new tube. The glass beads were washed with 500 μl lysis buffer,
532 centrifuged and the supernatant was added to the lysate. The lysate was sonicated six
533 to eight times for 10-15 seconds at 80% amplitude with one minute on ice between
534 each time. The sonicated material was centrifuged for 20 minutes at 2500 rpm. The
535 supernatant was used for immunoprecipitations (IP). The sonicated proteins were

pre-cleared with a 25µl protein A sepharose and protein G sepharose beads mixture (GE Healthcare) and the appropriate antibodies were added to the cleared extract and incubated overnight at 4°C. PCNA were immunoprecipitated with 2–5µg of anti-PCNA antibody (Sigma). A total of 10% of the extract was saved as input. The beads after the IP were washed once with lysis buffer, once with lysis buffer with 360 mM NaCl, once with washing buffer (10mM Tris/HCl pH8, 0.25M LiCl, 0.5% NP40, 0.5% Na-Deoxycholic acid, 1mM EDTA) and once with TE (10mM Tris/HCl pH8 and 10mM EDTA). The washed beads and the input were treated with elution buffer (50mM Tris/HCl pH8, 10mM EDTA, 1% SDS) overnight at 65°C. The DNA was precipitated, re-suspended in water and used for PCR real-time analysis(ABI StepOnePlusTM Real-Time PCR System); primer concentration and cycles number were calibrated individually for each reaction. All experiments are plotted as the average of at least three independent biological repeats and each biological repeat is the average of three technical PCR repeats. The oligonucleotides used are:

Y′-element 5′-GGCTTGATTTGGCAAACGTT-3′, and

5′-GTGAACCGCTACCATCAGCAT-3′.

ACKNOWLEDGEMENTS

We thank David Shore, Hele Ulrich, Connie Nugent, Michel Charboneau and Vicky Lundblad for strains and plasmids. We thank all present and past members of the Kupiec lab for support and ideas, and Ofir Hurvitz for help during the first stages of this project. This research was supported by grants from the Israel Science Foundation, the Israel Cancer Research Fund, and the Recanati Fund.

References

Arbel, M., Choudhary, K., Tfilin, O., & Kupiec, M. (2021). PCNA Loaders and Unloaders-One Ring That Rules Them All. *Genes (Basel), 12*(11). doi: 10.3390/genes12111812

Askree, S. H., Yehuda, T., Smolikov, S., Gurevich, R., Hawk, J., Coker, C., . . . McEachern, M. J. (2004). A genome-wide screen for Saccharomyces cerevisiae deletion mutants that affect telomere length. *Proc Natl Acad Sci U S A, 101*(23), 8658-8663. doi: 10.1073/pnas.0401263101

Bell, D. W., Sikdar, N., Lee, K. Y., Price, J. C., Chatterjee, R., Park, H. D., . . . Myung, K. (2011). Predisposition to cancer caused by genetic and functional defects of mammalian Atad5. *PLoS Genet, 7*(8), e1002245. doi: 10.1371/journal.pgen.1002245

Ben-Shitrit, T., Yosef, N., Shemesh, K., Sharan, R., Ruppin, E., & Kupiec, M. (2012). Systematic identification of gene annotation errors in the widely used yeast mutation collections. *Nat Methods, 9*(4), 373-378. doi: 10.1038/nmeth.1890

Bonnell, E., Pasquier, E., & Wellinger, R. J. (2021). Telomere Replication: Solving Multiple End Replication Problems. *Front Cell Dev Biol, 9*, 668171. doi: 10.3389/fcell.2021.668171

Chandra, A., Hughes, T. R., Nugent, C. I., & Lundblad, V. (2001). Cdc13 both positively and negatively regulates telomere replication. *Genes Dev, 15*(4), 404-414. doi: 10.1101/gad.861001

Chen, H., Xue, J., Churikov, D., Hass, E. P., Shi, S., Lemon, L. D., . . . Lei, M. (2018). Structural Insights into Yeast Telomerase Recruitment to Telomeres. *Cell, 172*(1-2), 331-343 e313. doi: 10.1016/j.cell.2017.12.008

Chen, L. Y., & Lingner, J. (2013). CST for the grand finale of telomere replication. *Nucleus, 4*(4), 277-282. doi: 10.4161/nucl.25701

de Lange, T. (2018). Shelterin-Mediated Telomere Protection. *Annu Rev Genet, 52*, 223-247. doi: 10.1146/annurev-genet-032918-021921

Evans, S. K., & Lundblad, V. (1999). Est1 and Cdc13 as comediators of telomerase access. *Science, 286*(5437), 117-120. doi: 10.1126/science.286.5437.117

Evans, S. K., & Lundblad, V. (2000). Positive and negative regulation of telomerase access to the telomere. *J Cell Sci, 113 Pt 19*, 3357-3364. doi: 10.1242/jcs.113.19.3357

Gao, H., Cervantes, R. B., Mandell, E. K., Otero, J. H., & Lundblad, V. (2007). RPA-like proteins mediate yeast telomere function. *Nat Struct Mol Biol, 14*(3), 208-214. doi: 10.1038/nsmb1205

Garg, M., Gurung, R. L., Mansoubi, S., Ahmed, J. O., Dave, A., Watts, F. Z., & Bianchi, A. (2014). Tpz1TPP1 SUMOylation reveals evolutionary conservation of SUMO-dependent Stn1 telomere association. *EMBO Rep, 15*(8), 871-877. doi: 10.15252/embr.201438919

Gatbonton, T., Imbesi, M., Nelson, M., Akey, J. M., Ruderfer, D. M., Kruglyak, L., . . . Bedalov, A. (2006). Telomere length as a quantitative trait: genome-wide survey and genetic mapping of telomere length-control genes in yeast. *PLoS Genet, 2*(3), e35. doi: 10.1371/journal.pgen.0020035

Ge, Y., Wu, Z., Chen, H., Zhong, Q., Shi, S., Li, G., . . . Lei, M. (2020). Structural insights into telomere protection and homeostasis regulation by yeast CST complex. *Nat Struct Mol Biol, 27*(8), 752-762. doi: 10.1038/s41594-020-0459-8

606 Grandin, N., Reed, S. I., & Charbonneau, M. (1997). Stn1, a new Saccharomyces cerevisiae protein,
607 is implicated in telomere size regulation in association with Cdc13. *Genes Dev, 11*(4), 512-
608 527. doi: 10.1101/gad.11.4.512
609 Grossi, S., Puglisi, A., Dmitriev, P. V., Lopes, M., & Shore, D. (2004). Pol12, the B subunit of DNA
610 polymerase alpha, functions in both telomere capping and length regulation. *Genes Dev,*
611 *18*(9), 992-1006. doi: 10.1101/gad.300004
612 Hang, L. E., Liu, X., Cheung, I., Yang, Y., & Zhao, X. (2011). SUMOylation regulates telomere length
613 homeostasis by targeting Cdc13. *Nat Struct Mol Biol, 18*(8), 920-926. doi:
614 10.1038/nsmb.2100
615 Harari, Y., & Kupiec, M. (2018). Mec1(ATR) is needed for extensive telomere elongation in
616 response to ethanol in yeast. *Curr Genet, 64*(1), 223-234. doi: 10.1007/s00294-017-0728-
617 1
618 Harari, Y., Romano, G. H., Ungar, L., & Kupiec, M. (2013). Nature vs nurture: interplay between
619 the genetic control of telomere length and environmental factors. *Cell Cycle, 12*(22),
620 3465-3470. doi: 10.4161/cc.26625
621 Harari, Y., Zadok-Laviel, S., & Kupiec, M. (2017). Long Telomeres Do Not Affect Cellular Fitness in
622 Yeast. *mBio, 8*(4). doi: 10.1128/mBio.01314-17
623 Hoege, C., Pfander, B., Moldovan, G. L., Pyrowolakis, G., & Jentsch, S. (2002). RAD6-dependent
624 DNA repair is linked to modification of PCNA by ubiquitin and SUMO. *Nature, 419*(6903),
625 135-141.
626 Hughes, T. R., Weilbaecher, R. G., Walterscheid, M., & Lundblad, V. (2000). Identification of the
627 single-strand telomeric DNA binding domain of the Saccharomyces cerevisiae Cdc13
628 protein. *Proc Natl Acad Sci U S A, 97*(12), 6457-6462. doi: 10.1073/pnas.97.12.6457
629 Itzkovich, Z., Choudhary, K., Arbel, M., & Kupiec, M. (2023). Effects of Defective Unloading and
630 Recycling of PCNA Revealed by the Analysis of ELG1 Mutants. *Int J Mol Sci, 24*(2). doi:
631 10.3390/ijms24021568
632 James, P., Halladay, J., & Craig, E. A. (1996). Genomic libraries and a host strain designed for highly
633 efficient two-hybrid selection in yeast. *Genetics, 144*(4), 1425-1436.
634 Jentsch, S., & Psakhye, I. (2013). Control of nuclear activities by substrate-selective and protein-
635 group SUMOylation. *Annu Rev Genet, 47*, 167-186. doi: 10.1146/annurev-genet-111212-
636 133453
637 Johnson, C., Gali, V. K., Takahashi, T. S., & Kubota, T. (2016). PCNA Retention on DNA into G2/M
638 Phase Causes Genome Instability in Cells Lacking Elg1. *Cell Rep, 16*(3), 684-695. doi:
639 10.1016/j.celrep.2016.06.030
640 Kang, M. S., Ryu, E., Lee, S. W., Park, J., Ha, N. Y., Ra, J. S., . . . Myung, K. (2019). Regulation of
641 PCNA cycling on replicating DNA by RFC and RFC-like complexes. *Nat Commun, 10*(1),
642 2420. doi: 10.1038/s41467-019-10376-w
643 Kim, S. J., Wie, M., Park, S. H., Kim, T. M., Park, J. H., Kim, S., . . . Lee, K. Y. (2020). ATAD5 suppresses
644 centrosome over-duplication by regulating UAF1 and ID1. *Cell Cycle, 19*(15), 1952-1968.
645 doi: 10.1080/15384101.2020.1785724
646 Kubota, T., Katou, Y., Nakato, R., Shirahige, K., & Donaldson, A. D. (2015). Replication-Coupled
647 PCNA Unloading by the Elg1 Complex Occurs Genome-wide and Requires Okazaki
648 Fragment Ligation. *Cell Rep, 12*(5), 774-787. doi: 10.1016/j.celrep.2015.06.066
649 Kubota, T., Nishimura, K., Kanemaki, M. T., & Donaldson, A. D. (2013). The Elg1 replication factor
650 C-like complex functions in PCNA unloading during DNA replication. *Mol Cell, 50*(2), 273-
651 280. doi: 10.1016/j.molcel.2013.02.012

652 Kuchenbaecker, K. B., Ramus, S. J., Tyrer, J., Lee, A., Shen, H. C., Beesley, J., . . . Brca. (2015).
653 Identification of six new susceptibility loci for invasive epithelial ovarian cancer. *Nat*
654 *Genet, 47*(2), 164-171. doi: 10.1038/ng.3185
655 Lim, C. J., Barbour, A. T., Zaug, A. J., Goodrich, K. J., McKay, A. E., Wuttke, D. S., & Cech, T. R. (2020).
656 The structure of human CST reveals a decameric assembly bound to telomeric DNA.
657 *Science, 368*(6495), 1081-1085. doi: 10.1126/science.aaz9649
658 Lin, J. J., & Zakian, V. A. (1996). The Saccharomyces CDC13 protein is a single-strand TG1-3
659 telomeric DNA-binding protein in vitro that affects telomere behavior in vivo. *Proc Natl*
660 *Acad Sci U S A, 93*(24), 13760-13765. doi: 10.1073/pnas.93.24.13760
661 Maicher, A., Gazy, I., Sharma, S., Marjavaara, L., Grinberg, G., Shemesh, K., . . . Kupiec, M. (2017).
662 Rnr1, but not Rnr3, facilitates the sustained telomerase-dependent elongation of
663 telomeres. *PLoS Genet, 13*(10), e1007082. doi: 10.1371/journal.pgen.1007082
664 Maleva Kostovska, I., Wang, J., Bogdanova, N., Schurmann, P., Bhuju, S., Geffers, R., . . . Dork, T.
665 (2016). Rare ATAD5 missense variants in breast and ovarian cancer patients. *Cancer Lett,*
666 *376*(1), 173-177. doi: 10.1016/j.canlet.2016.03.048
667 Matmati, S., Vaurs, M., Escandell, J. M., Maestroni, L., Nakamura, T. M., Ferreira, M. G., . . . Coulon,
668 S. (2018). The fission yeast Stn1-Ten1 complex limits telomerase activity via its SUMO-
669 interacting motif and promotes telomeres replication. *Sci Adv, 4*(5), eaar2740. doi:
670 10.1126/sciadv.aar2740
671 Mersaoui, S. Y., & Wellinger, R. J. (2019). Fine tuning the level of the Cdc13 telomere-capping
672 protein for maximal chromosome stability performance. *Curr Genet, 65*(1), 109-118. doi:
673 10.1007/s00294-018-0871-3
674 Miyagawa, K., Low, R. S., Santosa, V., Tsuji, H., Moser, B. A., Fujisawa, S., . . . Tanaka, K. (2014).
675 SUMOylation regulates telomere length by targeting the shelterin subunit Tpz1(Tpp1) to
676 modulate shelterin-Stn1 interaction in fission yeast. *Proc Natl Acad Sci U S A, 111*(16),
677 5950-5955. doi: 10.1073/pnas.1401359111
678 Nugent, C. I., Hughes, T. R., Lue, N. F., & Lundblad, V. (1996). Cdc13p: a single-strand telomeric
679 DNA-binding protein with a dual role in yeast telomere maintenance. *Science, 274*(5285),
680 249-252. doi: 10.1126/science.274.5285.249
681 Parker, J. L., Bielen, A. B., Dikic, I., & Ulrich, H. D. (2007). Contributions of ubiquitin- and PCNA-
682 binding domains to the activity of Polymerase eta in Saccharomyces cerevisiae. *Nucleic*
683 *Acids Res, 35*(3), 881-889. doi: 10.1093/nar/gkl1102
684 Parnas, O., Amishay, R., Liefshitz, B., Zipin-Roitman, A., & Kupiec, M. (2011). Elg1, the major
685 subunit of an alternative RFC complex, interacts with SUMO-processing proteins. *Cell*
686 *Cycle, 10*(17), 2894-2903. doi: 10.4161/cc.10.17.16778
687 Parnas, O., Zipin-Roitman, A., Pfander, B., Liefshitz, B., Mazor, Y., Ben-Aroya, S., . . . Kupiec, M.
688 (2010). Elg1, an alternative subunit of the RFC clamp loader, preferentially interacts with
689 SUMOylated PCNA. *Embo J, 29*(15), 2611-2622. doi: 10.1038/emboj.2010.128
690 Petreaca, R. C., Chiu, H. C., Eckelhoefer, H. A., Chuang, C., Xu, L., & Nugent, C. I. (2006).
691 Chromosome end protection plasticity revealed by Stn1p and Ten1p bypass of Cdc13p.
692 *Nat Cell Biol, 8*(7), 748-755. doi: 10.1038/ncb1430
693 Petreaca, R. C., Chiu, H. C., & Nugent, C. I. (2007). The role of Stn1p in Saccharomyces cerevisiae
694 telomere capping can be separated from its interaction with Cdc13p. *Genetics, 177*(3),
695 1459-1474. doi: 10.1534/genetics.107.078840
696 Puglisi, A., Bianchi, A., Lemmens, L., Damay, P., & Shore, D. (2008). Distinct roles for yeast Stn1 in
697 telomere capping and telomerase inhibition. *Embo J, 27*(17), 2328-2339. doi:
698 10.1038/emboj.2008.158

Rice, C., & Skordalakes, E. (2016). Structure and function of the telomeric CST complex. *Comput Struct Biotechnol J, 14*, 161-167. doi: 10.1016/j.csbj.2016.04.002

Rubinstein, L., Ungar, L., Harari, Y., Babin, V., Ben-Aroya, S., Merenyi, G., . . . Kupiec, M. (2014). Telomere length kinetics assay (TELKA) sorts the telomere length maintenance (tlm) mutants into functional groups. *Nucleic Acids Res, 42*(10), 6314-6325. doi: 10.1093/nar/gku267

Shemesh, K., Sebesta, M., Pacesa, M., Sau, S., Bronstein, A., Parnas, O., . . . Kupiec, M. (2017). A structure-function analysis of the yeast Elg1 protein reveals the importance of PCNA unloading in genome stability maintenance. *Nucleic Acids Res, 45*(6), 3189-3203. doi: 10.1093/nar/gkw1348

Shiomi, Y., & Nishitani, H. (2013). Alternative replication factor C protein, Elg1, maintains chromosome stability by regulating PCNA levels on chromatin. *Genes Cells, 18*(11), 946-959. doi: 10.1111/gtc.12087

Soudet, J., Jolivet, P., & Teixeira, M. T. (2014). Elucidation of the DNA end-replication problem in Saccharomyces cerevisiae. *Mol Cell, 53*(6), 954-964. doi: 10.1016/j.molcel.2014.02.030

Stelter, P., & Ulrich, H. D. (2003). Control of spontaneous and damage-induced mutagenesis by SUMO and ubiquitin conjugation. *Nature, 425*(6954), 188-191. doi: 10.1038/nature01965

Takahashi, T. S., Wollscheid, H. P., Lowther, J., & Ulrich, H. D. (2020). Effects of chain length and geometry on the activation of DNA damage bypass by polyubiquitylated PCNA. *Nucleic Acids Res, 48*(6), 3042-3052. doi: 10.1093/nar/gkaa053

Wang, M. J., Lin, Y. C., Pang, T. L., Lee, J. M., Chou, C. C., & Lin, J. J. (2000). Telomere-binding and Stn1p-interacting activities are required for the essential function of Saccharomyces cerevisiae Cdc13p. *Nucleic Acids Res, 28*(23), 4733-4741. doi: 10.1093/nar/28.23.4733

Yang, K., Moldovan, G. L., Vinciguerra, P., Murai, J., Takeda, S., & D'Andrea, A. D. (2011). Regulation of the Fanconi anemia pathway by a SUMO-like delivery network. *Genes Dev, 25*(17), 1847-1858. doi: 10.1101/gad.17020911

729 # Figure Legends

730 **Figure 1: SUMOylated PCNA regulates telomere length. A.** Southern blot (Teloblot)
731 showing that lack of SUMOylation of PCNA prevents telomere elongation.
732 Independently-created colonies were passaged ten times, its DNA extracted, digested
733 with *Xho*I and run in an agarose gel. The DNA was then transferred to a nitrocellulose
734 membrane, which was incubated with a radioactive probe that detects telomeres, and a
735 size marker. **B.** Teloblot showing that overexpression of wild type PCNA or Pol30-RR-
736 SUMO fusion, but not Pol30-ubiquitin fusion or Pol30-RR causes telomere elongation.

737

738 **Figure 2: Genetic and physical interaction between *ELG1* and *STN1.* A.** Teloblot
739 showing epistasis between *elg1*Δ and *stn1* mutants. **B.** Co-Immunoprecipitation
740 experiment showing physical interaction between Elg1 and Stn1 and reduced physical
741 interaction between Elg1-sim and Stn1. No interaction could be detected between Elg1
742 and Cdc13 or Ten1.

743 **Figure 3: Determinants of the Elg1-Stn1 interaction. A.** Schematic representation of the
744 Elg1 protein. The 3 SIM motifs, the WalkerA motif and the 2 threonines at the interface
745 with PCNA are shown. **B.** Yeast-Two-Hybrid (YTH) interaction of Cdc13 and Elg1 in a wild
746 type strain. AD: protein fused to the activating domain of Gal4; BD: protein fused to the
747 DNA binding domain of Gal4. e.v.: empty vector.**C.** YTH interaction of Stn1 and Elg1 in a
748 wild type strain. **D.** YTH experiments in the *siz1*Δ *siz2*Δ and *pol30-RR* background. **E.** Co-
749 Immunoprecipitation experiment showing physical interaction between Cdc13 and
750 PCNA.

751 **Figure 4: The unloading activity of Elg1 and Cdc13 SUMOylation are necessary for the**
752 **Elg1-Cdc13 interaction. A.** YTH experiment in a *elg1*Δ strain. **B.** YTH experiment in a
753 *elg1-sim* strain. **C.** YTH experiment in a *elg1-TT386/7DD* strain. **D.** YTH experiment in a
754 *elg1-sim+DD* strain. **E.** YTH experiment in a *elg1-Walker AB* strain. **F.** Lack of interaction
755 between *cdc13-snm* and Elg1 (in a wild type strain).

756 **Figure 5: Timing of Elg1-Stn1 interaction. A.** Co-IP experiment with synchronized cells.
757 Aliquots were taken at time intervals, Elg1 was immunoprecipitated, and the level of
758 Stn1 and Pol3 (the large subunit of DNA polymerase Delta) were monitored by Western
759 blot. Strains with single tags are shown as controls. Whole Cell Extract results are shown
760 in **Figure S5**. **B.** Quantitation of the Western shown in A. **C.** DNA content of the cells
761 used in A, by cell cytrometry. **D.** Chromatin immunoprecipitation at telomeres (Telo-
762 ChIP) in synchronized cells showing PCNA occupancy. **E.** Interaction between Stn1 and

763 Cdc13 in a wild type and a *elg1*Δ strain. **F.** Quantitation of three independent biological
764 repeats of the experiment shown in E. **:p<0.001.

765 **Figure 6: Model for the role of SUMOylated PCNA and Elg1 in telomere length**
766 **regulation. A.** Cdc13 binds ssDNA at the telomeres, Elg1 moves with the replisome at
767 the lagging strand, unloading PCNA in each Okazaki fragment. **B.** Arrival of the
768 SUMOylated PCNA at the fork to Cdc13 promotes telomerase activity. **C.** Elg1 interacts
769 with Stn1, which could be SUMOylated. Cdc13 becomes SUMOylated. Elg1 unloads
770 PCNA and leaves telomeres. **D.** Stn1 is now able to interact with Cdc13, evicting Est1 and
771 terminating telomerase activity.

772 **Figure S1: Weak interaction between Elg1 and Ten1.** Results of YTH experiments.

773 **Figure S2: Cdc13 interacts with PCNA, and mutations that prevent PCNA SUMOylation**
774 **(*pol30-RR*) also impair its interaction with Cdc13.**

775 **Figure S3: All *elg1* alleles used are expressed at similar levels.** Western blot results.

776 **Figure S4: A.** The *sumo-no-more* allele of Cdc13 has no effect on the YTH interactions
777 between wt Cdc13 or Stn1 and the N-terminus of Elg1. **B.** The C-terminus of Stn1
778 interacts with the N-terminus of Elg1 in wild type and *elg1*Δ strains.

779 **Figure S5:** Whole cell extract showing the level of Elg1, Stn1 and Pol3 in the cell cycle
780 experiment shown in **Figure 5**.

781

782 **Table 2: Yeast strains used in this study.**

Strain Number	*Name*	*Genotype*
13237	BY4741	*MATa his3del, leu2del, met15del, ura3del*
12480	*BY elg1Δ::HygMX*	*MATa his3del, leu2del, met15del, ura3del, elg1::HYG*
14421	*BY pol30-K127R*	*MATa his3del, leu2del, met15del, ura3del, pol30-K127R::LEU2*
14425	*BY pol30-K164R*	*MATa his3del, leu2del, met15del, ura3del, pol30-K164R::LEU2*
14423	*BY pol30-KK127,164RR*	*MATa his3del, leu2del, met15del, ura3del, pol30-RR::LEU2*
14426	*BY pol30-K127R elg1Δ*	*MATa his3del, leu2del, met15del, ura3del, pol30-K127R::LEU2, elg1::HYG*
14430	*BY pol30-K164R elg1Δ*	*MATa his3del, leu2del, met15del, ura3del, pol30-K164R::LEU2, elg1::HYG*
14428	*BY pol30-KK127,164RR elg1Δ*	*MATa his3del, leu2del, met15del, ura3del,pol30-RR::LEU2,elg1::HYG*
14398	*BY rad18Δ:: KanMX*	*MATa his3del, leu2del, met15del, ura3del, rad18::KanMX.*
14401	*BY rad18D::KanMX elg1D::HygMX*	*MATa his3del, leu2del, met15del, ura3del, rad18::KanMX, elg1::HYG*
19606	*BY pol30-KK127,164RR Elg1-HA*	*MATa his3del, leu2del, met15del, ura3del ELG1-HA-NAT pol30-KK127,164RR:HIS3*
20622	*BY bar1 CDC13-HA ELG1-HA*	*MATa his3del, leu2del, met15del, ura3del, bar1::LEU2, CDC13:3HA:HISMX, ELG1-HA-KanMX*
18418	*BY STN1-Myc Elg1-HA*	*MATa his3del, leu2del, met15del, ura3del stn1::HYG CEN LEU2 STN1-(G)9-(myc)7 ELG1-HA-KanMx*

18790	*BY bar1 STN1-Myc ELG1-HA POL3-FLAG*	*MATa his3del, leu2del, met15del, ura3del bar1::NatMX stn1::HYG CEN LEU2 STN1-(G)9-(myc)7 ELG1-HA-KanMx POL3-FLAG-URA3*
19552	*BY bar1 CDC13-HA POL30-FLAG*	*MATa his3del, leu2del, met15del ura3del, bar1:: NatMX CDC13-3HA::HISMX, POL30-FLAG::KanMX,*
20625	*BY CDC13-HA STN1-Myc*	*MATa his3del, leu2del, met15del, ura3del, CDC13-3HA::HISMX, stn1::HYG CEN LEU2 STN1-(G)9-(myc)7,*
20626	*BY CDC13-HA STN1-Myc elg1D*	*MATa his3del, leu2del, met15del, ura3del,CDC13-3HA::HISMX, stn1::HYG ,CEN LEU2 STN1-(G)9-(myc)7,elg1::KanMx*
20623	*BY TEN1-FLAG*	*MATa his3del, leu2del, met15del, ura3del trp1del Lys2del can1:: STE2pr-Sp_HIS5 ten1::KanMX, Elg1-HA-NAT CEN URA3 TEN1-(G)8-(FLAG)3*
17611	W303-1a	*MATa leu2-3, 112 ura3-1 his3-11,15, trp1-1, ade2-1, can1- 100*
9842	*W303 elg1Δ::HygMX*	*MATa leu2-3, 112 ura3-1 his3-11,15, trp1-1, ade2-1, can1- 100, elg1::KanMx*
9551	*W303 stn1-13*	*MATa leu2-3, 112 ura3-1 his3-11,15, trp1-1, ade2-1, can1- 100, stn1-13*
9848	*W303 elg1Δ::HygMX stn1-13*	*MATa leu2-3, 112 ura3-1 his3-11,15, trp1-1, ade2-1, can1- 100 elg1::KanMx, stn1-13*
12357	*W303 stn1-164*	*MATa leu2-3, 112 ura3-1 his3-11,15, trp1-1, ade2-1, can1- 100, stn1Δ::Hyg + pRS-stn1-L164A (pVL3571)*
12358	*W303 stn1-164 elg1Δ: KanMX*	*MATa leu2-3, 112 ura3-1 his3-11,15, trp1-1, ade2-1, can1- 100, elg1::KanMx, stn1Δ::Hyg+pRS-stn1-L164A (pVL3571)*

12062	PJ69-4	*MAT@ trp1-901 leu2-3,112 ura3-52 his3-200 gal4del gal80del GAL2-ADE2 LYS2:: GAL1-HIS3 met2::GAL7-lacZ*
15017	*PJ elg1D*	*MAT@ trp1-901 leu2-3,112 ura3-52 his3-200 gal4del gal80del GAL2-ADE2 LYS2:: GAL1-HIS3 met2::GAL7-lacZ elg1::HYG*
19774	*PJ siz1 siz2*	*MAT@ trp1-901 leu2-3,112 ura3-52 his3-200 gal4del gal80del GAL2-ADE2 LYS2:: GAL1-HIS3 met2::GAL7-lacZ siz1::KanMX siz2::HYG*
11069	*PJ pol30-RR*	*MAT@ trp1-901 leu2-3,112 ura3-52 his3-200 gal4del gal80del GAL2-ADE2 LYS2:: GAL1-HIS3 met2::GAL7-lacZ POL30-RR :: leu2 :: KANMX*
20624	*PJ STN1-Myc*	*MAT@ trp1-901 leu2-3,112 ura3-52 his3-200 gal4del gal80del GAL2-ADE2 LYS2:: GAL1-HIS3 met2::GAL7-lacZ elg1-sim::KanMx, stn1::HYG,CENLEU2 STN1-(G)9-(myc)7*
19916	*PJ elg1-sim-Myc*	*MAT@ trp1-901 leu2-3,112 ura3-52 his3-200 gal4del gal80del GAL2-ADE2 LYS2:: GAL1-HIS3 met2::GAL7-lacZ elg1-SIM-MYC-KANMX*
18798	*PJ elg1-DDMyc*	*MAT@ trp1-901 leu2-3,112 ura3-52 his3-200 gal4del gal80del GAL2-ADE2 LYS2:: GAL1-HIS3 met2::GAL7-lacZ elg1-DD-MYC-KANMX*
19917	*PJ elg1-DD+sim-Myc*	*MAT@ trp1-901 leu2-3,112 ura3-52 his3-200 gal4del gal80del GAL2-ADE2 LYS2:: GAL1-HIS3 met2::GAL7-lacZ elg1-DDsim-MYC-KANMX*
19915	*PJ elg1-Walker A*	*MAT@ trp1-901 leu2-3,112 ura3-52 his3-200 gal4del gal80del GAL2-ADE2 LYS2:: GAL1-HIS3 met2::GAL7-lacZ, elg1 KK343/4DD:MYC:KanMX*
19486	*PJ cdc13-snm*	*MAT@ trp1-901 leu2-3,112 ura3-52 his3-200 gal4del gal80del GAL2-ADE2 LYS2:: GAL1-HIS3 met2::GAL7-lacZ cdc13-snm*

783

787 **Table 3: Plasmids used in this study**

Strain Number	Genotype	Source or Reference
4239	pGad424 (LEU2)	Kupiec lab
4238	pGad424-POL30	Helle Ulrich lab
4237	pGad424-pol30-k127r,k164r	Helle Ulrich lab
4236	pGad424-pol30-k127r,k164r-SMT3	Helle Ulrich lab
4235	pGAD424-pol30-k127r,k164r-UBI	Helle Ulrich lab
4147	CEN LEU2 STN1-(G)9-(myc)7	Victoria Lundblad lab
4144	CEN URA3 TEN1-(G)8-(FLAG)3	Victoria Lundblad lab
2201	pCN181 pACT2-STN1 (LEU2)	Constance Nugent lab
2205	pVL855 pACT2-CDC13	Constance Nugent lab
2168	pACT2 - TEN1	Michel Charbonneau lab
1775	pGBU9 (URA3)	Kupiec lab
1973	pGBU9-ELG1-NTD(1-234)	This Study
3301	pGBU9-ELG1-CTD(541-791)	This Study
2260	pGBU9-ELG1-NTDsim(1-234)	This Study
2241	pGBU9-SMT3	This Study
2419	pGAD424-Stn1-Nt(1-282)	David Shore lab
2420	pGAD424-Stn1-Ct(282-494)	David Shore lab
2169	pGAD424-Stn1-13	Michel Charbonneau lab
2418	pGAD424-Stn1-63	David Shore lab
4287	pACT-cdc13-snm	This Study

788

789

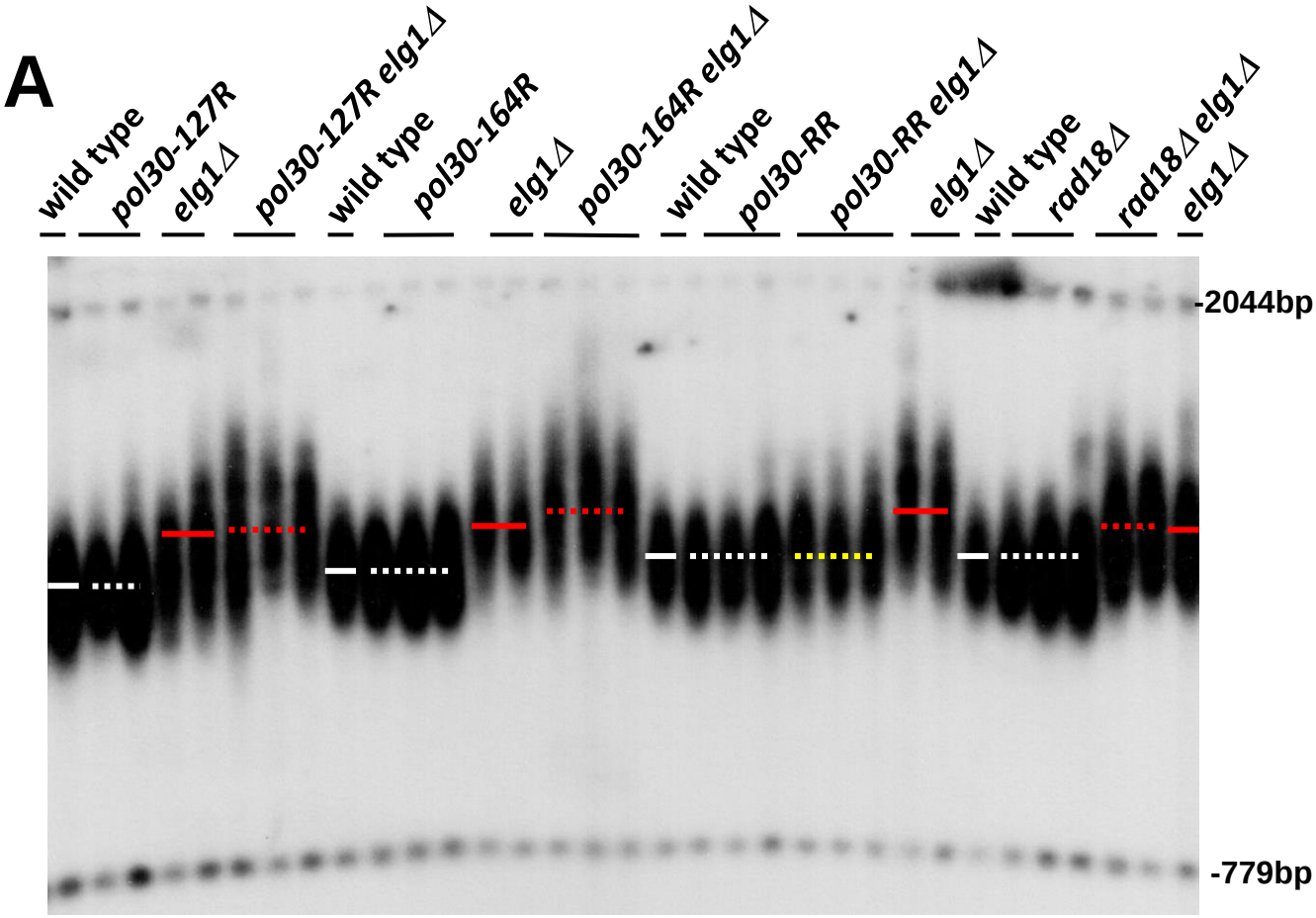
A
wild type
pol30-127R
elg1Δ
pol30-127R elg1Δ
wild type
pol30-164R
elg1Δ
pol30-164R elg1Δ
wild type
pol30-RR
pol30-RR elg1Δ
elg1Δ
wild type
rad18Δ
rad18Δ elg1Δ
elg1Δ
-2044bp
-779bp

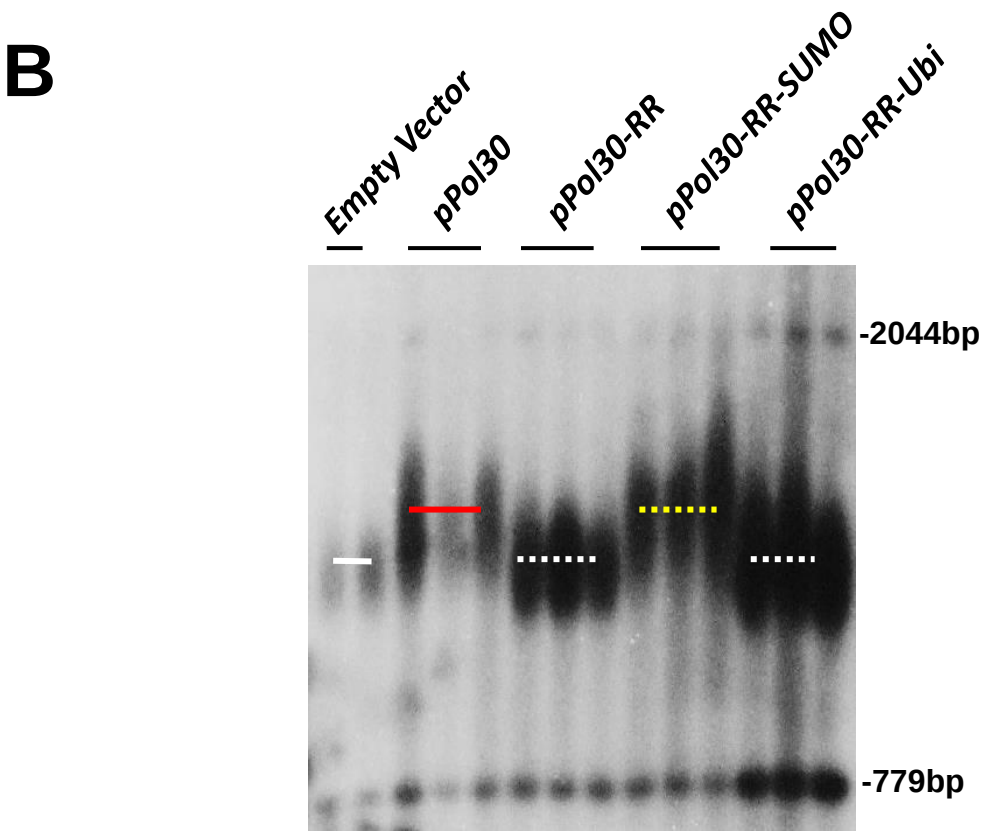
B
Empty Vector
pPol30
pPol30-RR
pPol30-RR-SUMO
pPol30-RR-Ubi
-2044bp
-779bp

Figure1

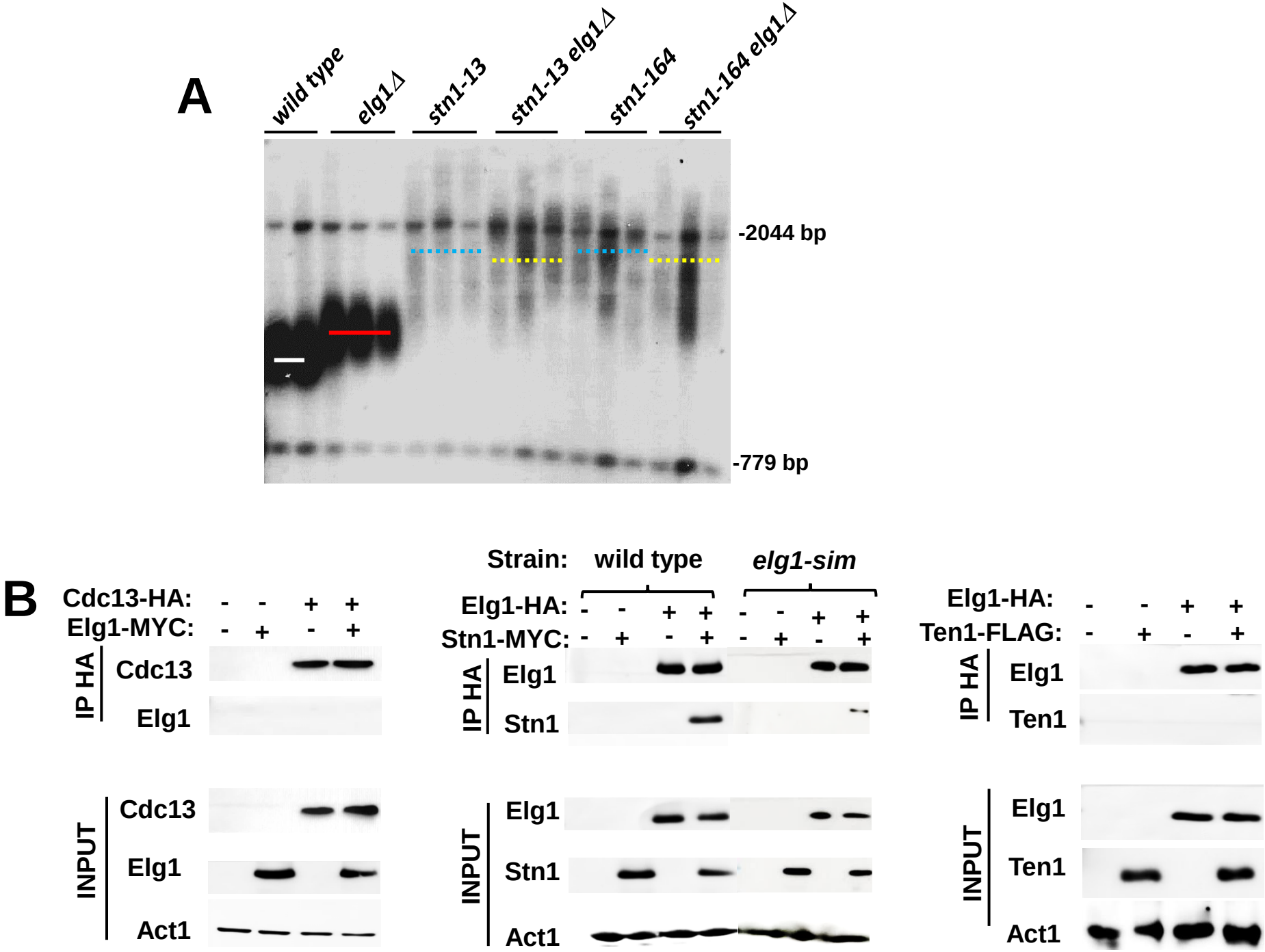
A
wild type
elg1Δ
stn1-13
stn1-13 elg1Δ
stn1-164
stn1-164 elg1Δ
-2044 bp
-779 bp
B
Cdc13-HA:
Elg1-MYC:
IP HA
Cdc13
Elg1
INPUT
Cdc13
Elg1
Act1
Strain:
wild type
elg1-sim
Elg1-HA:
Stn1-MYC:
IP HA
Elg1
Stn1
INPUT
Elg1
Stn1
Act1
Elg1-HA:
Ten1-FLAG:
IP HA
Elg1
Ten1
INPUT
Elg1
Ten1
Act1

Figure 2

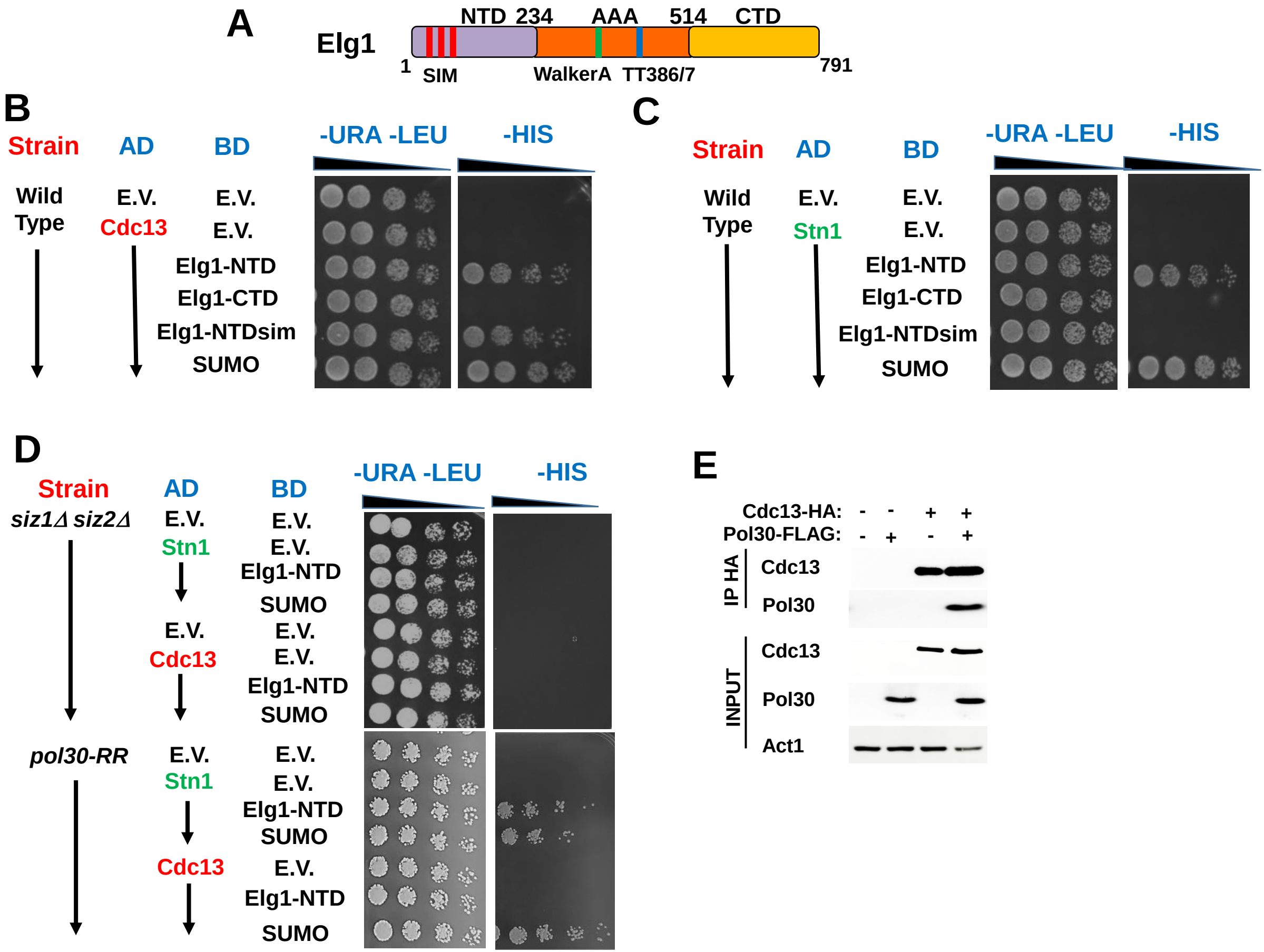
A
Elg1
NTD 234
AAA
514
CTD
1
SIM
WalkerA
TT386/7
791
B
Strain
AD
BD
-URA -LEU
-HIS
Wild Type
E.V.
E.V.
Cdc13
E.V.
Elg1-NTD
Elg1-CTD
Elg1-NTDsim
SUMO
C
Strain
AD
BD
-URA -LEU
-HIS
Wild Type
E.V.
E.V.
Stn1
E.V.
Elg1-NTD
Elg1-CTD
Elg1-NTDsim
SUMO
D
Strain
AD
BD
-URA -LEU
-HIS
siz1Δ siz2Δ
E.V.
E.V.
Stn1
E.V.
Elg1-NTD
SUMO
E.V.
E.V.
Cdc13
E.V.
Elg1-NTD
SUMO
pol30-RR
E.V.
E.V.
Stn1
E.V.
Elg1-NTD
SUMO
Cdc13
E.V.
Elg1-NTD
SUMO
E
Cdc13-HA: - - + +
Pol30-FLAG: - + - +
IP HA
Cdc13
Pol30
INPUT
Cdc13
Pol30
Act1

Figure 3

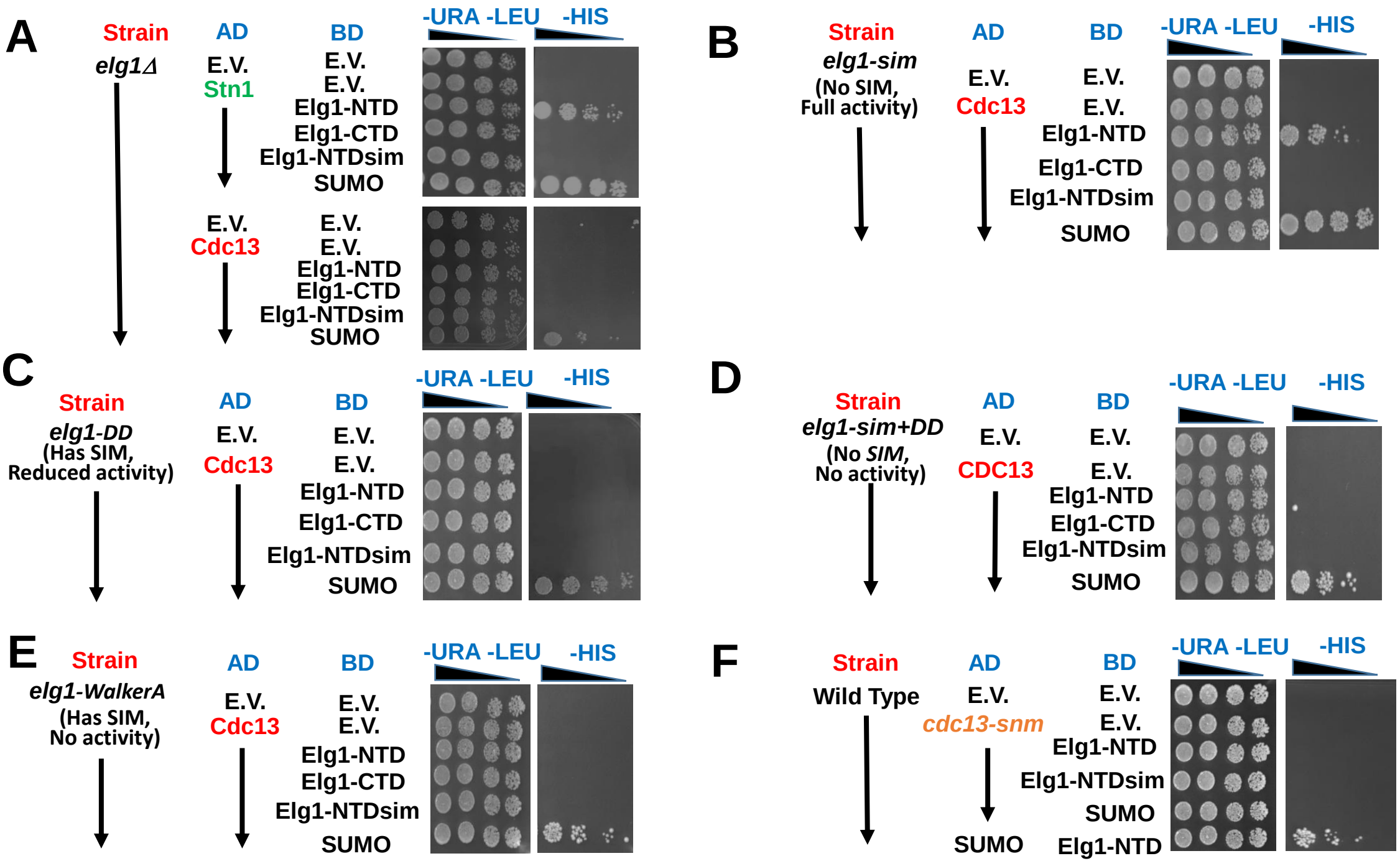
A
Strain
elg1Δ
AD
E.V.
Stn1
E.V.
Cdc13
BD
E.V.
E.V.
Elg1-NTD
Elg1-CTD
Elg1-NTDsim
SUMO
E.V.
E.V.
Elg1-NTD
Elg1-CTD
Elg1-NTDsim
SUMO
-URA -LEU
-HIS
B
Strain
elg1-sim
(No SIM,
Full activity)
AD
E.V.
Cdc13
BD
E.V.
E.V.
Elg1-NTD
Elg1-CTD
Elg1-NTDsim
SUMO
-URA -LEU
-HIS
C
Strain
elg1-DD
(Has SIM,
Reduced activity)
AD
E.V.
Cdc13
BD
E.V.
E.V.
Elg1-NTD
Elg1-CTD
Elg1-NTDsim
SUMO
-URA -LEU
-HIS
D
Strain
elg1-sim+DD
(No SIM,
No activity)
AD
E.V.
CDC13
BD
E.V.
E.V.
Elg1-NTD
Elg1-CTD
Elg1-NTDsim
SUMO
-URA -LEU
-HIS
E
Strain
elg1-WalkerA
(Has SIM,
No activity)
AD
E.V.
Cdc13
BD
E.V.
E.V.
Elg1-NTD
Elg1-CTD
Elg1-NTDsim
SUMO
-URA -LEU
-HIS
F
Strain
Wild Type
AD
E.V.
cdc13-snm
SUMO
BD
E.V.
E.V.
Elg1-NTD
Elg1-NTDsim
SUMO
Elg1-NTD
-URA -LEU
-HIS

Figure 4

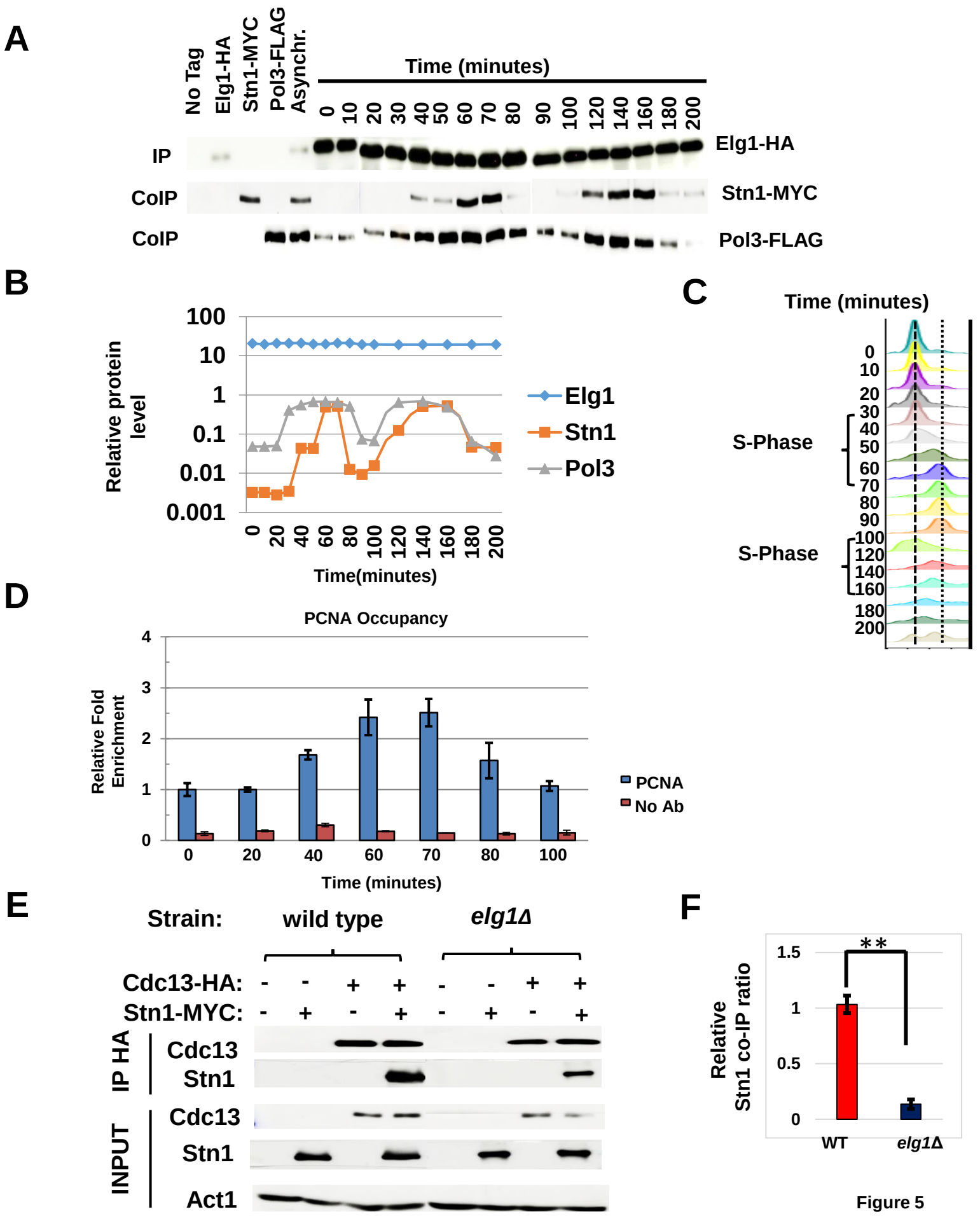
A
No Tag
Elg1-HA
Stn1-MYC
Pol3-FLAG
Asynchr.
Time (minutes)
0 10 20 30 40 50 60 70 80 90 100 120 140 160 180 200
IP
CoIP
CoIP
Elg1-HA
Stn1-MYC
Pol3-FLAG
B
Relative protein level
100
10
1
0.1
0.01
0.001
0 20 40 60 80 100 120 140 160 180 200
Time(minutes)
Elg1
Stn1
Pol3
C
Time (minutes)
0
10
20
30
40
50
60
70
80
90
100
120
140
160
180
200
S-Phase
S-Phase
D
PCNA Occupancy
Relative Fold Enrichment
4
3
2
1
0
0 20 40 60 70 80 100
Time (minutes)
PCNA
No Ab
E
Strain:
wild type
elg1Δ
Cdc13-HA: - - + + - - + +
Stn1-MYC: - + - + - + - +
IP HA
Cdc13
Stn1
INPUT
Cdc13
Stn1
Act1
F
Relative Stn1 co-IP ratio
1.5
1
0.5
0
**
WT
elg1Δ

Figure 5

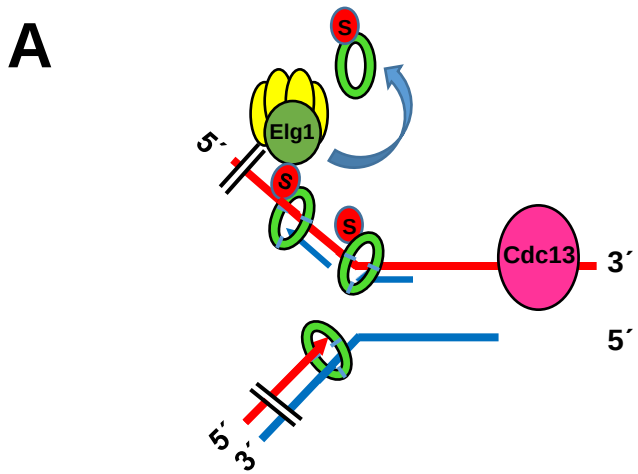

Last origin firing: Elg1 moves with the fork towards the telomeres and unloads S-PCNA.

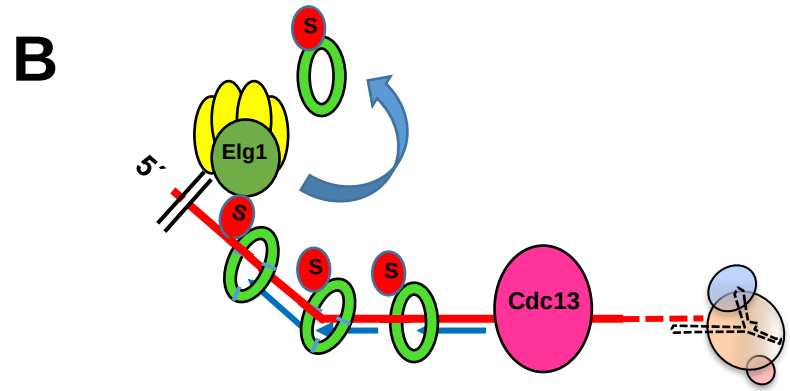

Arrival of S-PCNA with the fork to telomeres leads to the activation of telomerase and to telomere elongation.

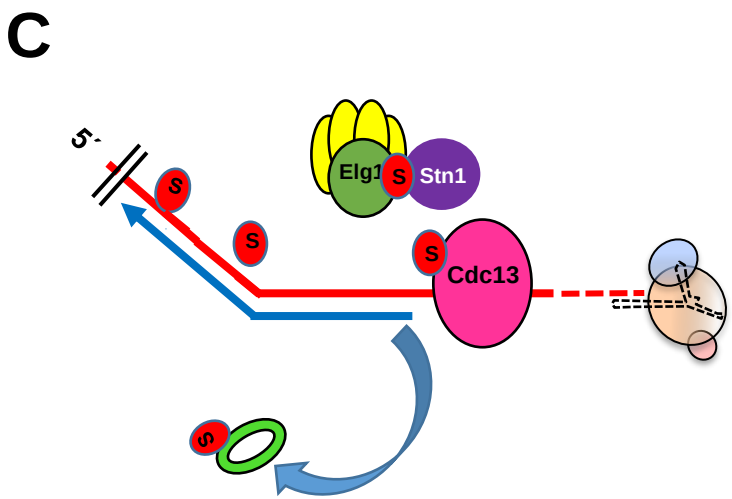

Elg1 interacts with S-Stn1. Elg1 unloads PCNA, Cdc13 becomes SUMOylated.

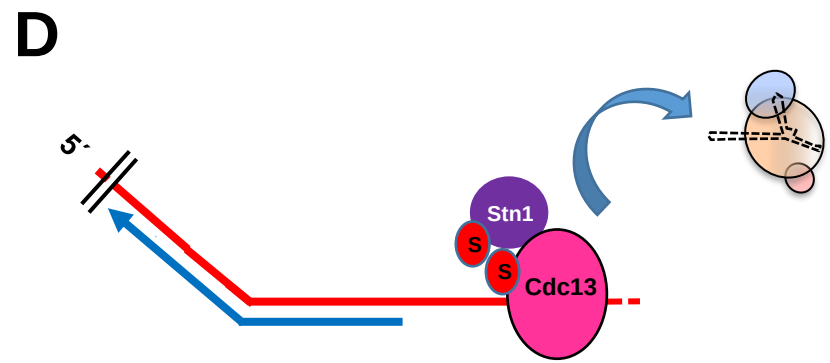

Stn1 (and presumably Ten1) binds SUMOylated Cdc13, terminating telomerase activity.

Figure 6